Neurobiology of Stress 14 (2021) 100324

Contents lists available at ScienceDirect

Neurobiology of Stress

journal homepage: www.elsevier.com/locate/ynstr

Resilience to anhedonia-passive coping induced by early life experience is linked to a long-lasting reduction of I_h current in VTA dopaminergic neurons

Sebastian Luca D'Addario [a,b,c,2], Matteo Di Segni [b,2], Ada Ledonne [b], Rosamaria Piscitelli [b,d], Lucy Babicola [a,b], Alessandro Martini [b], Elena Spoleti [e,3], Camilla Mancini [f], Donald Ielpo [a,b,c], Francesca R. D'Amato [g], Diego Andolina [a,b], Davide Ragozzino [b,e], Nicola B. Mercuri [b,h], Carlo Cifani [f], Massimiliano Renzi [e], Ezia Guatteo [b,d,**,1], Rossella Ventura [a,b,*,1]

[a] Dept. of Psychology and Center "Daniel Bovet", Sapienza University, Rome, Italy
[b] IRCCS Fondazione Santa Lucia, Roma, Italy
[c] Behavioral Neuroscience PhD Programme, Sapienza University, Piazzale Aldo Moro, 5 00184, Rome, Italy
[d] Dept. of Motor Science and Wellness, 'Parthenope' University, Via Medina 40, 80133 Naples, Italy
[e] Department of Physiology and Pharmacology, Sapienza University, Rome, 00185, Italy
[f] University of Camerino School of Pharmaceutical Sciences and Health Products, Camerino, Italy
[g] Biochemistry and Cell Biology Institute, National Research Council, Via E Ramarini 32, 00015, Monterotondo Scalo, Roma, Italy
[h] Dept. of Systems Medicine, Tor Vergata University, 00133, Rome, Italy

ARTICLE INFO

Keywords:
Early stress
I_h current
VTA
Resilience
In vivo pharmacology

ABSTRACT

Exposure to aversive events during sensitive developmental periods can affect the preferential coping strategy adopted by individuals later in life, leading to either stress-related psychiatric disorders, including depression, or to well-adaptation to future adversity and sources of stress, a behavior phenotype termed "resilience".

We have previously shown that interfering with the development of mother-pups bond with the Repeated Cross Fostering (RCF) stress protocol can induce resilience to depression-like phenotype in adult C57BL/6J female mice. Here, we used patch-clamp recording in midbrain slice combined with both *in vivo* and *ex vivo* pharmacology to test our hypothesis of a link between electrophysiological modifications of dopaminergic neurons in the intermediate Ventral Tegmental Area (VTA) of RCF animals and behavioral resilience. We found reduced hyperpolarization-activated (I_h) cation current amplitude and evoked firing in VTA dopaminergic neurons from both young and adult RCF female mice. *In vivo*, VTA-specific pharmacological manipulation of the I_h current reverted the pro-resilient phenotype in adult early-stressed mice or mimicked behavioral resilience in adult control animals.

This is the first evidence showing how pro-resilience behavior induced by early events is linked to a long-lasting reduction of I_h current and excitability in VTA dopaminergic neurons.

1. Introduction

Genetic and environmental factors contribute in a complex manner to the aetiology of most psychiatric disorders, operatively defined through their phenotypical dysfunctional coping responses to internal and external stimuli (APA, 2013).

* Corresponding author. Dept. of Psychology and Center "Daniel Bovet", Sapienza University, 00184 Rome, IRCCS Fondazione Santa Lucia, via del Fosso di Fiorano, 64, 00143, Roma, Italy.
** Corresponding author. Dept. of Motor Science and Wellness, 'Parthenope' University, Via Medina 40, 80133 Napoli, IRCCS Fondazione Santa Lucia, via del Fosso di Fiorano, 64, 00143, Roma, Italy.
E-mail addresses: ezia.guatteo@uniparthenope.it (E. Guatteo), rossella.ventura@uniroma1.it (R. Ventura).
[1] Ezia Guatteo and Rossella Ventura share last authorship.
[2] Sebastian Luca D'Addario and Matteo Di Segni contributed equally to this work.
[3] Current address: Department of Medicine, Campus-Biomedico, Rome 00128, Italy.

https://doi.org/10.1016/j.ynstr.2021.100324
Received 19 December 2020; Received in revised form 24 February 2021; Accepted 27 March 2021

Clinical and preclinical research highlighted how exposure to aversive events during sensitive developmental periods can affect the preferential coping strategy adopted by individuals later in life, thus representing a risk factor for the development of stress-related psychiatric disorders, including depression (Heim and Nemeroff, 2002; Caspi et al., 2010; Heim et al., 2008; Pechtel and Pizzagalli, 2011; Heim and Binder, 2012; Gershon et al., 2013; Schmitt et al., 2014; Andersen, 2015; Herbison et al., 2017; Novick et al., 2018; Rokita et al., 2018; Santarelli et al., 2014, 2017; Di Segni et al., 2019, 2020; Torres-Berrío et al., 2019; Song and Gleeson, 2018). Yet, the same critical early-life experiences can differently affect brain development trajectories and behavioral coping strategies depending on individual's characteristics (Daskalakis et al., 2013; Belsky and Pluess, 2009, 2013; Ellis et al., 2011; Santarelli et al., 2017; Belsky et al., 2015; Di Segni et al., 2016, 2017, 2019; Song and Gleeson, 2018; Torres-Berrío et al., 2019). In fact, both clinical and preclinical studies report that early aversive experiences might even result in protective effects Daskalakis et al. (2013); Nederhof and Schmidt (2012); Schmidt (2011); Santarelli (2017); Gururajan et al. (2019) by promoting well-adaptation to future adversity and sources of stress – a behavioral phenotype termed "resilience" (APA, 2013).

Functional imaging and postmortem tissue analysis from depressed patients have identified abnormalities in several, distinct regions of the human brain (Liotti et al., 2001; Nestler et al., 2002; Drysdale et al., 2017; Torres-Berrìo et al., 2019). Intriguingly, among these is the 'reward pathway' (Tye et al., 2013; Fox and Lobo, 2019), whose dysregulation is thought to be involved in the loss of pleasure and amotivational syndrome observed in depressed patients (Belujon and Grace, 2017). Thus, the mesocorticolimbic circuitry is now considered as one of the neural substrates of depression-related behaviors and a possible target for antidepressant treatments (Nestler and Carlezon, 2006; Chaudhury et al., 2013; Mayberg et al., 2005; Tye et al., 2013; Luo et al., 2019; Ku and Han, 2017; Puglisi-Allegra and Ventura, 2012; Di Segni et al., 2016; Slattery and Cryan, 2017; Belujon & Grace, 2014, 2017).

Within the motivation and reward circuitry, a key role is played by the Ventral Tegmental Area (VTA), the mesencephalic area from which the mesocorticolimbic dopaminergic (DAergic) system reaches both cortical and sub-cortical projection targets (Kumar et al., 2018; Blood et al., 2010; Kaufling, 2019; Douma and de Kloet, 2020; Han et al., 2019; Lammel et al., 2014; Penã et al., 2017; 2019). Interestingly, VTA undergoes adaptations in depressed patients as well as in animal models of depression-like behavior (Kumar et al., 2018; Blood et al., 2010; Kaufling, 2019; Douma and de Kloet, 2020; Han et al., 2019; Lammel et al., 2014; Rincón-Cortés and Grace, 2017), and recent reports suggest this brain area to be associated with both vulnerability and resilience to depression (Tye et al., 2013; Fox and Lobo, 2019; Han et al., 2019; Douma and de Kloet, 2020; Luo et al., 2019; Kaufling, 2019; Cao et al., 2010; Friedman et al., 2014, 2016; Zhong 2018; Zhang et al., 2019; Cheng et al., 2019).

Similar to humans, in rodents the development of DAergic mesolimbic pathways seems to be largely sensitive to early life experiences (Meaney et al., 2002; Brake et al., 2004; Peña et al., 2017, 2019). The first 2 weeks of life seem to be particularly critical in rodents to shape the DAergic circuitry of the adult brain (Gillies et al., 2014) and stress factors occurring early in life can induce transcriptional, structural and functional modifications in the VTA (Chocyk et al., 2011; Authement et al., 2015; Penã et al., 2019; Masrouri et al., 2020; Shepard et al., 2020; Spyrka et al., 2020). In a nutshell, early experiences may impact the VTA and its DAergic network, thus influencing stress coping strategies and susceptibility or resilience to depression in adulthood.

To understand how the VTA is associated with vulnerability or resilience to depression-like behaviors, the preclinical field is deeply investigating molecular and physiological changes occurring in VTA neurons of susceptible and resilient animals (Tye et al., 2013; Fox and Lobo, 2019; Han et al., 2019; Douma and de Kloet, 2020; Luo et al., 2019; Kaufling, 2019; Cao et al., 2010; Friedman et al., 2014, 2016; Zhong 2018; Zhang et al., 2019; Cheng et al., 2019; Isingrini et al., 2016; Chaundhury et al., 2013; Spyrka et al., 2020; Ku et al., 2017; Masrouri et al., 2020).

VTA dopamine (DA) neurons display complex functional patterns (for reviews, see Morikawa and Paladini 2011; Paladini and Roeper 2014; Marinelli et al., 2006; Kaufling 2019; Tapia et al., 2018) regulated by a sophisticated excitatory/inhibitory synaptic input balance and by intrinsic electrophysiological characteristics leading to a peculiar firing activity which regulates DA release in target areas (Tye et al., 2013; Fox and Lobo, 2019; Han et al., 2019; Douma and de Kloet, 2020; Luo et al., 2019; Kaufling, 2019).

Among several regulating factors, the activity of VTA DA neurons is governed by multiple voltage-dependent ionic conductances, including the hyperpolarization-activated cation current 'I_h', mediated by hyperpolarization-activated cyclic nucleotide gated (HCN) channels (McDaid et al., 2008; Okamoto et al., 2006; Migliore and Migliore 2012; Ku and Han, 2017; Carbone et al., 2017; Krashia et al., 2017). HCN channels are widely expressed in the mesocorticolimbic system (Chu and Zhen, 2010; Santoro and Shah, 2020), with HCN2 being the predominant subunit expressed in the VTA (Notomi and Shigemoto, 2004; Santos-Vera et al., 2019; Zhong et al., 2018).

A few of seminal works (Cao et al., 2010; Tye et al., 2013; Friedman et al., 2014; Zhong et al., 2018; Zhang et al., 2019; Cheng et al., 2019) have recently unveiled relevant adaptations in the VTA DA neurons of depression-susceptible or -resilient animals following chronic stress exposure in adulthood. For instance, I_h current and firing activity of VTA DA neurons were found altered in animal models of chronic stress-induced depression as well as in depression-resilient mice (Tye et al., 2013; Friedman et al., 2014; Zhong et al., 2018; Masrouri et al., 2020; Isingrini et al., 2016; Chaundhury et al., 2013; Spyrka et al., 2020; Ku et al., 2017).

We have previously demonstrated that exposure to an early life experience interfering with the mother-pups bond development (Repeated Cross Fostering; RCF) induces in adult C57BL/6J (C57) female mice increased resilience to depression-like phenotype, consisting in increased active coping behavior in the forced swimming test (FST) as well as enhanced preference for a natural rewarding stimulus (saccharin preference test, SPT; Di Segni et al., 2016; 2017) while increases depression-like behavior in C57 males (Di Segni et al., 2019). It is important to underline that the RCF protocol does not necessary represent a stress, as basal and stress-induced corticosterone levels were not different between RCF and control adult animals (D'Amato et al., 2011; Di Segni et al., 2016; 2019). This early manipulation is, instead, aimed to interfere with mother-pups attachment bond (D'Amato et al., 2011; Ventura et al., 2013; Di Segni et al., 2016; 2017; 2018; 2019; 2020).

Interestingly, we could relate the pro-resilient behavioral pattern observed in female mice to the altered release of catecholamines within the mesocorticolimbic DAergic system in response to rewarding and aversive stimuli (Ventura et al., 2013; Di Segni et al., 2016, 2017, 2018, 2020). However, a detailed characterization of the functional modifications of VTA DAergic neurons in this model of early life adversity and the possible link to behavioral alterations later in life is currently missing. Here, we investigated the electrophysiological properties of VTA DA neurons from juvenile or adult RCF *vs.* control mice to understand the neuroadaptations underlying the behavioral resilience observed in early-manipulated animals. Further, with an *in vivo* and *ex vivo* pharmacological approach, we tested the hypothesis that such resilience might be associated to the altered electrophysiological properties found in RCF VTA DA neurons.

2. Materials and methods

2.1. Animals

C57BL/6J (C57) female mice (Charles River Laboratories, Italy) were housed with water and food available ad libitum, at constant room

temperature (21 ± 1 °C) and in a 12:12 h light–dark cycle (lights on at 07:00 a.m.). Adequate measures were taken to minimize pain or discomfort of mice and all experiments were carried out in accordance with Italian national laws (DL 116/92 and DL 26/2014) on the use of animals for research based on the European Communities Council Directives (86/609/EEC and 2010/63/UE). Experimental protocol (no. 769/2017) was approved by Italian Ministry of Health. Mice 9–10 weeks old (below referred to as 'P60') were used for both behavioral and electrophysiological experiments. In addition, 2 groups of 16–22 days old RCF and Control mice were used for patch-clamp recordings.

2.2. Repeated cross-fostering (RCF)

As previously described (D'Amato et al., 2011; Ventura et al., 2013; Di Segni et al., 2016) pups from the same litter spent the first postnatal day (P0) with their biological mother. On P1, litters were randomly assigned to experimental (RCF) or Control (CTRL) group. RCF pups were fostered by moving the entire litter into the home cage of a different mother, whose pups had just been moved to an adoptive mother. This procedure was repeated daily (since P1 until P4); on P4 pups were left with the last adoptive mother until weaning. Control litters were only picked up daily and reintroduced in their home cage; this procedure was carried out within 30 s. Animals were weaned at P28, separated by sex and housed in groups of 4 littermates. To prevent potential estrous cycle group synchronization, experimental subjects for cross-fostered and Control female groups were sorted by collecting max 2 individuals per cage/litter (Ventura et al., 2013; Di Segni et al., 2016, 2017, 2019).

2.3. Drugs

Zoletil 100 (tiletamine HCl 50 mg/ml + zolazepam HCl 50 mg/ml; from Virbac, Italy) and Rompun 20 (xylazine 20 mg/ml; from Bayer S. p. A, Italy) were dissolved in saline solution (4.1 mg/ml and 1.6 mg/ml, respectively) prior injection (7.3 ml/kg). 4-(N-Ethyl-N-phenylamino)-1,2 dimethyl-6-(methylamino) pyrimidinium chloride (ZD7288; from Hello Bio, UK) was dissolved in 0.9% NaCl and 6-(2,3-Dichlorophenyl)-1,2,4-triazine-3,5-diamine (Lamotrigine; from Hello Bio, UK) was dissolved in DMSO. All drugs used for electrophysiology were prepared from thawed concentrated stocks (Abcam or Sigma) and either bath applied at final concentration in artificial cerebrospinal fluid (below) via a three-way tap syringe or, where specified, dissolved in the pipette solution.

2.4. Stereotaxic injection into the VTA

Animals were anesthetized with Zoletil and Rompun and positioned in a stereotaxic frame (David Kopf Instruments, CA, USA) equipped with a mouse adapter. For behavioral experiments, mice were chronically implanted bilaterally with a 26-gauge guide cannula positioned 1 mm from the VTA using the following coordinates (from brain surface): AP = − 3.2, ML = 0.4, DV = − 3.6 mm (Cao et al., 2010). After 5–7 days of post-operative recovery, ZD7288 (ZD; 0.1 μg in NaCL 0.9%) or Lamotrigine (LTG; 0.1 μg in DMSO) were bilaterally injected (ZD: 4 consecutive days; LTG: 5 consecutive days) through an injector cannula in a total volume 0.4 μl/side at a continuous rate of 0.15 μl/min under the control of a micro-infusion pump. Concentrations of ZD and LTG were chosen based on previous works (Cao et al., 2010; Friedman et al., 2014; Zhong et al., 2018; Chevaleyre and Castillo, 2002; Kocsis and Li, 2004). Control groups were infused with drug vehicle only. The injector cannula was removed 5 min after the end of infusion to prevent backflow. Mice were returned to their home cage and tested after 24h. The same procedure was used for both behavioral and electrophysiology experiments.

2.5. Electrophysiology

2.5.1. Midbrain slice preparation

Horizontal midbrain slices containing the VTA (250 μm; VT1200S, Leica Biosystems) were prepared according to recently published procedures (Martini et al., 2019; Lo Iacono et al., 2018; Krashia et al., 2017; Ledonne and Mercuri, 2018; Ting et al., 2018). Briefly, young (P16-22) or adult (P60) C57BL6 female mice, previously exposed to RCF or control manipulations (CTRL), were anesthetized with halothane and quickly decapitated. Brains were removed from the skull and a tissue block containing the midbrain was isolated and placed in chilled bubbled (95% O_2–5% CO_2) standard artificial cerebrospinal fluid (aCSF) at 8–10 °C (P16-22 or young mice) containing (in mM): NaCl 126, $NaHCO_3$ 24, glucose 10, KCl 2.5, $CaCl_2$ 2.4, NaH_2PO_4 1.2 and $MgCl_2$ 1.2 (pH 7.4; ~290 mOsm), or a low-sodium N-methyl-D-glucamine (NMDG)-based aCSF at 2–4 °C (P > 60, or adult mice), containing (in mM): 92 NMDG, 2.5 KCl, 1.25 NaH_2PO_4, 30 $NaHCO_3$, 20 HEPES, 25 glucose, 2 thiourea, 5 Na-ascorbate, 3 Na-pyruvate, 0.5 $CaCl_2$, and 10 $MgSO_4$ (pH to 7.3–7.4 with 18% hydrochloric acid).

After cutting procedures, slices from young mice (P16-22) were maintained in standard aCSF (32–33 °C) for at least 30 min prior to usage, whereas slices from adult mice (P60) were maintained in a baker filled with 150 mL of NMDG-based aCSF at 33.0 ± 0.5 °C for 5 min, before adding progressively increasing volumes of a sodium-spike solution (2M NaCl in NMDG-based aCSF; Ting et al., 2018) every 5 min: 250 μL, 250 μL, 500 μL, 1000 μL, 2000 μL. Five minutes after the last addition, slices were transferred in a HEPES-based aCSF for long-term storage, containing (in mM): 92 NaCl, 2.5 KCl, 1.25 NaH_2PO_4, 30 $NaHCO_3$, 20 HEPES, 25 glucose, 2 thiourea, 5 Na-ascorbate, 3 Na-pyruvate, 2 $CaCl_2$, and 2 $MgSO_4$ (95% O2–5% CO2; pH 7.3–7.4). Slices from adult mice were let recovering for at least 1 h before being transferred in the recording chamber for the electrophysiological recordings, where they were continuously perfused at 2.5–4 mL/min with normal aCSF (33.0 ± 0.5 °C), containing (in mM): NaCl 126, $NaHCO_3$ 24, glucose 10, KCl 2.5, $CaCl_2$ 2.4, NaH_2PO_4 1.2 and $MgCl_2$ 1.2, saturated with 95% O_2–5% CO_2 (pH 7.4; ~290 mOsm).

2.5.2. Electrophysiological recordings

A single slice was placed into a recording chamber (0.6 mL) of an upright microscope (BX51WI; Olympus; Nikon or DMLSF; Leica) and continuously perfused (2.5 or 3–4 ml/min) with aCSF saturated with a 95% O2, 5% CO_2 gas mixture. Pipettes were pulled from thin-walled capillaries to a final tip resistance of 5–6 MΩand filled with an 'intracellular' solution containing (in mM): 125 K-gluconate, 10 KCl, 10 HEPES, 2 $MgCl_2$, 4 ATP-Mg_2, 0.3 GTP-Na_3, 0.75 EGTA, 0.1 $CaCl_2$, 10 Phosphocreatine-Na_2 (pH 7.2, ~280 mOsm). Cell-attached and whole-cell patch-clamp recordings of VTA DA neurons (MultiClamp 700B and Digidata 1322A; Molecular Devices) were performed from visually identified neurons (40X) selected by the following criteria: 1) location in the intermediate region of the VTA (iVTA), according to the practical map we recently described (Krashia et al., 2017); 2) presence of low-frequency, regular firing of action potentials (APs) in cell-attached configuration; 3) presence of I_h current (see Tab. 2 in Krashia et al., 2017). These criteria were validated using transgenic mice expressing eGFP under the gene promoter for Tyrosine Hydroxylase (TH, the rate-limiting enzyme in dopamine synthesis typical of DA neurons) or by *post-hoc* TH immunostaining on sample recorded neurons (data not shown; Ungless et al., 2004; Chaudhury et al., 2013; Krashia et al., 2017; Zhong et al., 2018). All recordings were performed at 32–34 °C with no liquid junction potential correction.

Spontaneous firing (0.5–5 Hz) was recorded in cell-attached configuration (unless otherwise stated) to avoid cytoplasm dialysis by pipette solution, as soon as a ≥1 GΩ seal resistance was achieved and just before membrane rupture (V_H − 60 mV; amplifier in-built 8-pole low-pass Bessel filter, f_c 3 kHz; sampling 20 kHz). Membrane resistance (R_m) and whole-cell capacitance (C_m) were measured within 2 min

after membrane rupture using the in-built Clampex 9 'membrane test' protocol, consisting of a 30 ms-long, − 5 mV step from V_H − 60 mV (33.3 Hz). A mean of 20 consecutive measurements was used to calculate final values. Access resistance (R_s) was monitored and recordings with $R_s > 20$ MΩ were discarded. Hyperpolarization-activated inward current (I_h) was recorded in whole-cell in response to hyperpolarizing voltage steps (1 sec-long; from −60 to − 120 mV, 20 mV increment, V_H − 60 mV; f_c 2 kHz; sampling 10 kHz).

To analyze neuronal excitability, a current-clamp configuration protocol consisting in 1- or 2-s current steps from 0 to 0.2 nA (or from −0.2 to 0.4 nA in experiments on LTG-treated slices; 50 pA increments) was delivered to VTA DA neurons, while maintaining their membrane potential at $V_H = -60$ mV with current injection. Mean number of action potentials (APs) evoked by each current step was obtained by averaging results from three stimulation protocols (f_c 10 kHz; sampling 50 kHz; no drugs added to the aCSF).

To analyze voltage-gated K+channel-mediated currents, a voltage-clamp protocol consisting in 4-s long step voltages (from −70 mV to + 20 mV, increment of 10 mV) was delivered to VTA DA neurons ($V_H = -70$ mV) in the presence of tetrodotoxin (1 μM), $CdCl_2$ (200 μM), kynurenic acid (1 mM) and picrotoxin (100 μM).

To analyze evoked glutamatergic synaptic transmission, a glass-pipette monopolar electrode was placed 100–200 μm rostral to the VTA DA neuron recorded and excitatory postsynaptic currents (EPSCs) were evoked by delivering brief electrical pulses (100–200 μs duration, every 30 s) through a constant current isolated stimulating unit (Digitimer, UK), with stimulation settings adjusted to induce currents of 100–300 pA amplitude. AMPAR-EPSCs or NMDAR-EPSCs were pharmacologically isolated in the presence of the $GABA_A$ antagonist Picrotoxin (100 μM), plus the NMDAR antagonist APV (50 μM) or the AMPAR antagonist NBQX (20 μM), respectively. Evoked EPSCs were recorded using a Cs-Methansulphonate-based solution, containing (in mM): 115 Cs-Methanesulphonate, 10 CsCl, 0.45 $CaCl_2$, 1 EGTA, 10 HEPES, 5 QX-314-Cl, 0.3 Na_3GTP, 4 MgATP, 10 Phosphocreatine (pH 7.2, ~280 mOsm).

AMPA/NMDA ratios were calculated from AMPAR- and NMDAR-peak EPSC amplitudes (both recorded at $V_H = +40$ mV). AMPAR- and NMDAR-mediated currents were pharmacologically isolated and subsequently quantified following digital subtraction.

The rectification index of AMPARs was obtained as: AMPAR-EPSC peak amplitude at $V_H = -70$ mV/AMPAR-EPSC peak amplitude at $V_H = +40$ mV, with spermine (0.1 mM) added to the intracellular Cs-Methansulphonate-based solution and NMDAR-mediated currents pharmacologically blocked. The possible modulation of NMDAR subunit composition, specifically affecting GluN2B expression, was evaluated by analyzing NMDAR-EPSC sensitivity to the GluN2B subunit-selective antagonist Ifenprodil (applied at 3 μM for 30 min).

For experiments aimed at investigating the effect of intra-VTA injection of the I_h blocker ZD7288 (ZD) or the I_h enhancer Lamotrigine (LTG; see below for details on the *in vivo* drug infusion protocol) either behavioral tests or *ex vivo* slice recordings were performed 24 h after last drug injection.

2.5.3. Data analysis

Analysis of current-clamp and voltage-clamp recordings was performed using Clampfit (Molecular Devices), Origin (Version, 2019 Pro; OriginLab, Northampton, MA), Sigma Plot and Igor. Pro 6.32A (WaveMetrics Inc.) with NeuroMatic 2.8 (Rothman and Silver, 2018).

The neuron approximate resting potential (RP) was estimated using the amplifier inbuilt voltmeter immediately after accessing the cell interior. The input resistance (R_{in}) was estimated as the slope of a linear least-squares fit to the relationship between the amplitude of five sub-threshold steps of injected currents (range: 0.20–0 nA; 1 s duration; cells held at – 60 mV) and the steady-state voltage response of the cell (Suter et al., 2013). To investigate cell excitability, the rheobase (the amplitude of the injected current necessary to induce the first AP) was estimated (Clampfit) from the voltage response to a series of 5 pA-incremental consecutive steps of I_{inj} (50 ms duration; range: 0–0.4 nA). To quantify the AP threshold (V_{thre}), phase-plane plots of dV_m/dt versus V_m ('phase plots') were built for the first AP induced during the rheobase protocol. Spike threshold was estimated as the membrane potential value at which dV_m/dt increased suddenly and developed with a monotonic rise (Bean 2007; Trombin et al., 2011). To study evoked excitability, curves describing the relationship between the frequency of evoked APs and the amplitude of current injections (f – I relationships) were compared. Detection of APs was performed in Clampfit or in NeuroMatic using a threshold crossing method.

The amplitude of I_h current was measured at the current steady-state and after nulling the current baseline at the interception between the offset of the capacitive peak and the onset of the hyperpolarization-activated inward current, for each step response (Krashia et al., 2017).

2.6. Western Blotting

Brain tissue micro-punches of the VTA region were obtained from frozen ≤300 μm-thick coronal brain slices according to the Paxinos and Franklin brain atlas (2019) using stainless-steel tubes of 0.5 mm inner diameter and stored at − 80 °C (Patrono et al., 2015). On the day of the assay, single frozen VTA punches were lysate by brief sonication in 40 μl of Lysis buffer (20 mM Tris pH 7.4, 1 mM EDTA, 1 mM EGTA, 1% Triton X-100; 4 °C) and then centrifuged at 12,000 g (4 °C for 30 min). Finally, the supernatant was removed and stored at – 80 °C and protein concentration was determined by Bradford assay (Biorad). 15 μg of protein lysates were boiled for 5 min at 95 °C after addition of sample buffer (0.5 M Tris, 30% glycerol, 10% SDS, 0.6 M dithio-threitol, 0.012% bromophenol blue). Proteins were separated by electrophoresis on 10% acrylamide/bisacrylamide gels and transferred electrophoretically to nitrocellulose membranes, which were then blocked for 1 h at room temperature in Tris-buffered saline (in mM: 137 NaCl and 20 Tris-HCl, pH 7.5) containing 0.1% Tween 20 (TBS-T) and 5% low-fat milk (Bio--Rad), as previously described (Andolina et al., 2018).

Membranes were incubated at 4 °C overnight with primary antibodies diluted in TBS-T with 1% low-fat milk (1:1000 mouse monoclonal anti-HNC2 from Abcam; 1:5000 rabbit policlonal anti-beta actine from Genetex), washed extensively in TBS-T and incubated (1 h, room temperature) with HRP-linked secondary antibodies (anti-mouse and anti-rabbit IgG, respectively, diluted 1:8000 in TBS-T with 5% low-fat milk; Immunological Sciences). Chemioluminescent signals (ECL-R; Amersham) were digitally scanned by ChemiDoc (Bio-Rad) and quantified using densitometric image software (ImageJ 64); HCN2 signal was normalized to beta-actine.

2.7. Behavioral tests

2.7.1. Saccharin preference test (SPT)

The saccharin preference test was carried out as previously described with minor modifications (Di Segni et al., 2016, 2019). During the habituation day, animals were singly moved in a cage with two bottles containing water; after 24h they were exposed to a double choice drinking test (saccharin solution 0.5% or drinking water) from graduated tubes (10 ml volume). Intake was measured to the nearest 0.1 ml. The test cage was the same throughout the experiment. Only mice drinking at least 0.1 ml on day 1 were included in the study. The percentage of saccharin intake (saccharin intake (ml) *100/saccharin + H 20 intake (ml)) was evaluated.

2.7.2. Forced Swim Test (FST)

Mice were individually placed in an 18 cm-diameter glass cylinder (height 40 cm) filled with 20 cm of water at 28 ± 2 °C as previously described (Ventura et al., 2013; Di Segni et al., 2016, 2019). Behavioral response was video-recorded for 10 min using a digital camera placed in the front of the apparatus before returning the mice to the home cage.

The duration (in sec) of immobility was taken as dependent variable and was manually scored using the "EthoVision" software (Noldus, The Netherlands) by a trained observer blind to the animals' treatment.

2.7.3. Tail Suspension Test (TST)

Each mouse was suspended by the tail at 60 cm above the floor in a white plastic chamber using adhesive tape placed < 1 cm from the tip of the tail according to Yan et al., (2015). Behavior was recorded for 10 min using a digital camera placed in the front of the apparatus. The duration of immobility was manually scored using the "EthoVision" software (Noldus, The Netherlands) by a trained observer blind to the animals' treatment. In this test, the *immobility* was defined as the period when the animals stopped struggling for ≥1 s.

2.8. Statistical analysis

Statistical analysis of behavioral data was performed using MATLAB software (v. R2019a, Mathworks MA, USA). One sample Student's *t* -test was performed on the time spent in immobility during FST and TST (treatment: ZD or LTG *vs* Vehicle). Saccharin preference test was analyzed by repeated-measures ANOVA with one *between* factor (treatment: ZD or LTG *vs* Vehicle) and one *within* factor (intake (%): Saccharin, H_2O). *Post-hoc* analysis was performed when appropriated. Western Blotting data were analyzed by Student's *t* -test.

Statistical analysis of patch-clamp data was run in Sigma Plot, Prism 6 (GraphPad) or OriginPro using Mann–Whitney *U* test, unpaired Student's *t* -tests (with Welch's correction), one-way or two-way repeated measures ANOVA with Bonferroni's test for *post-hoc* analysis, as required. Normality of data sets was valuated using either Shapiro–Wilk test or D'Agostino & Pearson omnibus normality test. $P < 0.05$ was considered significant. Data are expressed as average values ± SEM.

3. Results

3.1. RCF affects *functional properties of VTA DA neurons of young female mice*

We aimed at investigating if RCF, a protocol of early life adversity (D'Amato et al., 2011, Ventura et al., 2013; Di Segni et al., 2016; 2017), could cause in resilient female mice (Di Segni et al., 2016, 2019) permanent functional alteration(s) in DA neurons of the intermediate VTA (iVTA), an area of the mesocorticolimbic pathway projecting, among others, to the Nucleus Accumbens (NAc; Lammel et al., 2011; Krashia et al., 2017) and involved in the reward circuitry. Firstly, we evaluated electrophysiological properties of iVTA DA neurons in young (P16-22) CTRL and RCF mice, as this age represents a critical period for the maturation of the DAergic innervation. In current-clamp experiments we found that membrane resistance (R_m) was lower in RCF compared to CTRL VTA neurons (CTRL, 277 ± 16 MΩ and RCF, 217 ± 11 MΩ, both n = 20, Student's *t* -test: $t = 3.14$, df = 33, $p < 0.01$; Fig. 1A). Interestingly, no difference in R_m was found across groups when a Cs-based pipette solution was used, suggesting that the modulation of a K^+ conductance was involved in the alteration observed (for CTRL and RCF respectively: 485 ± 38 MΩ, n = 42 and 535 ± 38 MΩ, n = 30, Student's *t* -test: $t = -0.925$, df = 68.2, $p = 0.358$; Fig. 1A). Besides the reduction in R_m, both whole-cell capacitance (C_m) and spontaneous AP firing frequency (FF, recorded in cell-attached) were unaltered (for C_m Student's *t* -test: $t = -1.38$, df = 61.9, $p = 0.17$; and for FF $t = 0.28$, df = 14.18, $p = 0.77$; Fig. 1B and C).

The hyperpolarization-activated current I_h is a hallmark of VTA DA neurons (Grace and Onn, 1989; Mercuri et al., 1995), with amplitude typically decreasing from lateral to medial regions (Krashia et al., 2017) and found to be sensitive to stress experiences (Friedman et al., 2014; Zhong et al., 2018) as well as to neurological diseases (He et al., 2014; Di Francesco and Di Francesco, 2015; Guatteo et al., 2017). Thus, in voltage-clamp experiments we explored the effects of the early stress protocol on I_h in DA neurons of the iVTA and found that indeed the current amplitude was significantly lower in neurons from RCF mice (two-way repeated measure ANOVA: $F_{(1,19)} = 8.71$, $p = 0.0082$, n = 20 for both experimental groups). In particular, Bonferroni's *post-hoc* analysis revealed that I_h currents from RCF mice were significantly smaller than CTRL at the most negative potentials applied: at V_H − 60 mV, CTRL −5.8 ± 0.8 pA, RCF −6.2 ± 0.8 pA, $p = 1$; at V_H − 80 mV, CTRL −35 ± 6 pA, RCF −25 ± 3 pA, $p = 1$; at V_H − 100 mV, CTRL – 80 ± 10 pA, RCF – 55 ± 6 pA, $p = 0.037$; at V_H – 120 mV, CTRL – 109 ± 11 pA, RCF – 71 ± 8 pA, $p = 1.71 \times 10^{-4}$, Fig. 1D). These data suggest that RCF alters the sub-threshold properties of iVTA neurons along the maturation of DAergic projections in young mice.

Because stressful events affects the glutamatergic transmission onto VTA DA neurons (Bellone et al., 2011) and the maturation also involves the formation of excitatory inputs from prefrontal cortex and other brainstem nuclei to VTA neurons, we aimed at investigating if RCF affected the glutamatergic transmission onto iVTA neurons from young mice (P16-22).

Firstly, we investigated possible RCF-induced changes in AMPAR/NMDAR ratio, i.e. the ratio between AMPAR- and NMDAR-mediated excitatory postsynaptic currents (AMPAR-EPSCs and NMDAR-EPSCs, respectively). We found no significant differences in the AMPA/NMDA ratio between the two experimental groups (CTRL 0.30 ± 0.04, n = 8, and RCF 0.31 ± 0.05, n = 9; Student's *t* -test, $t = -0.104$, df = 14.56, $p = 0.91$; Fig. 1E), indicating that RCF does not induce general modifications in the evoked glutamatergic synaptic transmission in iVTA DA neurons. To address possible RCF-induced alterations in AMPAR and NMDAR functional properties that might stay undetected when evaluating the AMPAR/NMDAR ratio, we investigated AMPAR- or NMDAR-mediated synaptic transmission separately. In particular, we analyzed the rectification index (RI) of AMPAR-EPSCs in VTA DA neurons of RCF or CTRL midbrain slices and found similar values (RI close to 1, indicative of channel conductance linearity): CTRL, 0.94 ± 0.08, n = 6, and RCF, 1.07 ± 0.09, n = 7; Student's *t* -test, $t = -1.02$, df = 14.55, $p = 0.32$; Fig. 1F). As the RI depends on the receptor subunit composition, our results suggest lack of modifications of AMPAR subunit composition and channel conductance by the early stressful experience. Further, NMDARs in VTA DA neurons at mature stage express GluN2B subunits whose expression and contribution to NMDAR-EPSCs is considered an index of glutamatergic synapse maturation (Bellone et al., 2011). To investigate whether RCF altered NMDAR composition and GluN2B expression, we analyzed NMDAR-EPSCs sensitivity to ifenprodil, a subunit-specific GluN2B antagonist. We found that NMDAR-EPSCs in VTA DA neurons from RCF- or CTRL slices were similarly reduced by Ifenprodil (3 μM, 30 min): the residual NMDAR-EPSCs (% of baseline at the steady-state of block) was 70 ± 5% in CTRL (n = 8) and 69 ± 8% in RCF (n = 9) and, Student's *t* -test, t = 0.14, df = 13.58, $p = 0.88$ (Fig. 1G), thus suggesting that RCF does not alter synaptic NMDARs composition in VTA DA neurons of young mice.

Overall, these results show that RCF does not alter glutamatergic synaptic transmission in VTA DA neurons nor cause a detectable delay in glutamatergic synapse maturation.

3.2. RCF-dependent alteration of VTA DA neurons persists into adulthood

We have previously shown that RCF produces distinct and divergent phenotypes in C57 mice depending on the sex, increasing anhedonia and depression-related behaviors in adult males, and promoting pro-resilient phenotype in females (Di Segni et al., 2019).

We then asked whether the functional modifications induced by RCF in DA neurons of young female mice persisted throughout adulthood. To address this, we performed voltage- and current-clamp measures on intermediate VTA neurons in slices from RCF and CTRL adult animals (P60) and found that the alterations observed in young animals were still present in adults. Thus, the R_m of RCF iVTA DA neurons from P60 mice was strongly reduced (CTRL, 287 ± 15 MΩ and RCF 237 ± 15 MΩ,

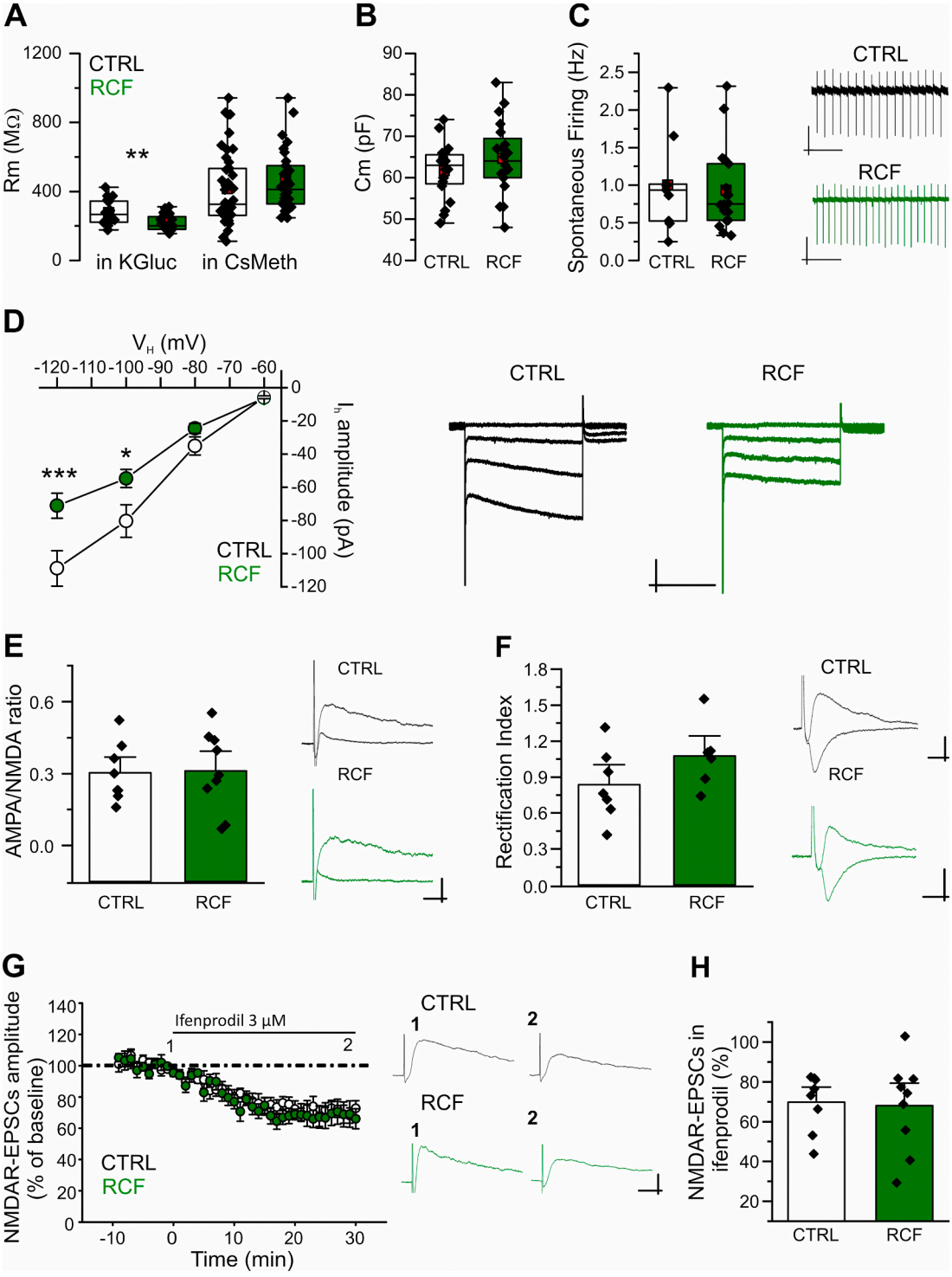

(caption on next page)

Fig. 1. Young RCF female mice show altered R_m and I_h in DA neurons of the iVTA *A*, Membrane resistance (R_m) of DA neurons in the iVTA from RCF mice (P16-22) is significantly lower compared to Control mice in presence of intracellular K^+ (left panel), but not with intracellular Cs^+ (right panel). With K^+_i, CTRL 277 ± 16 MΩ and RCF 217 ± 11 MΩ (both n = 20; Student *t*-test, t = 3.14, df = 33.04,**$p < 0.01$); with Cs^+_i, CTRL 485 ± 38 MΩ and RCF 535 ± 38 MΩ (42 and 30 cells, respectively; t = −0.925, df = 68.2, $p = 0.358$). *B*, Lack of difference in membrane capacitance (C_m) across conditions: CTRL 70 ± 4 pF and RCF 76 ± 3 pF (35 and 29 cells, respectively; Student's *t* -test: t = −1.38, df = 61.9, $p = 0.17$). *C*, Lack of difference across conditions in spontaneous AP firing: CTRL 1.0 ± 0.2 Hz and RCF 0.9 ± 0.1 Hz (9 and 18 cells, respectively; $t = 0.28$, df = 14.18, $p = 0.77$; inset: example cell-attached recordings). Scale bars: upper 10 pA, 4 s; lower 5 pA, 4 s. *D*, Current (pA) – to – Voltage (mV) relationship depicting significant reduction of I_h amplitude in VTA neurons from RCF mice (left). For the I–V relationship the two-way repeated measure ANOVA analysis returned: for '*in vivo* treatment' (i.e. RCF vs CTR) $F_{(1,19)} = 8.71$, **$p = 0.0082$; and for 'membrane potential' (V_H) $F_{(3,17)} = 56.5$, ***$p = 4.73 \times 10^{-}9$; with the interaction treatment x membrane potential $F_{(3,17)} = 3.016$, $p = 0.0586$. The Bonferroni's *post-hoc* analysis returned: at V_H − 60 mV, CTRL −5.8 ± 0.8 pA, RCF −6.2 ± 0.8 pA, $p = 1$; at V_H − 80 mV, CTRL −35 ± 6 pA, RCF −25 ± 3 pA, $p = 1$; at V_H − 100 mV, CTRL – 80 ± 10 pA, RCF – 55 ± 6 pA, *$p = 0.037$; at V_H – 120 mV, CTRL – 109 ± 11 pA, RCF – 71 ± 8 pA, ***$p = 1.71 \times 10^{-4}$ (n = 20 for each condition). To the right, typical I_h currents recorded from CTRL or RCF neurons in response to command voltage steps (four consecutive sweeps superimposed). Scale bars: 100 pA, 0.5 s. *E*, Lack of difference across conditions for the AMPA/NMDA ratio of evoked EPSCs from iVTA DA neurons (left, bar plots of pooled data; right, typical traces): CTRL 0.30 ± 0.04 and RCF 0.31 ± 0.05 (8 and 9 cells, respectively; $p = 0.91$). Scale bars: 100 pA, 50 ms. *F*, Rectification index of synaptic AMPARs is not altered in iVTA DA neurons from RCF mice respect to CTRL, as depicted in bar plots of pooled data (left) and representative traces (right): CTRL 0.94 ± 0.08 and RCF 1.07 ± 0.09 (13 and 7 cells, respectively; $p = 0.32$). Scale bars: 100 pA, 50 ms. *G*, Effect of the GluN2B antagonist ifenprodil on evoked NMDAR-mediated EPSCs showing similar sensitivity across conditions. Left, time-course of evoked NMDAR-mediated EPSCs (amplitudes were normalized to the baseline) before and during bath application of ifenprodil (3 μM). Middle, representative NMDAR-EPSC currents before (1) and 25–30 min after (2) ifenprodil application. Scale bars: 100 pA, 50 ms. Right, bar plots of residual NMDAR-EPSCs amplitude (% of baseline) showing similar sensitivity to ifenprodil in CTRL and RCF iVTA DA neurons: CTR 70 ± 5% and RCF 69 ± 8% (8 and 9 cells, respectively; $p = 0.88$).

n = 28 and 19, respectively; Student's *t* -test: $t = 2.38$, df = 43.86, $p < 0.05$; Fig. 2A), whereas again whole-cell capacitance and spontaneous firing were unaltered (for C_m, Student's *t* -test: $t = 1.63$, df = 42.16, $p = 0.11$, CTRL n = 28, RCF n = 19; for FF, Student's *t* -test: $t = 0.62$, df = 22.02, $p = 0.54$, CTRL, n = 13, RCF, n = 19; Fig. 2B and C). Similarly to P16-22, RCF caused in adult animals a strong reduction of I_h amplitude at the most negative voltage commands, as revealed by two-way repeated measures ANOVA ($F_{(1,15)} = 10.49$, $p = 0.0055$) and Bonferroni's *post-hoc* analysis: at V_H – 60 mV, CTRL – 6.8 ± 0.7 pA, RCF – 6 ± 1 pA, $p = 1$; at V_H – 80 mV, CTRL – 69 ± 9 pA, RCF – 42 ± 5 pA, $p = 1$; at V_H – 100 mV, CTRL – 168 ± 17 pA, RCF – 104 ± 9 pA, $p = 0.0015$; at V_H – 120 mV, CTRL – 233 ± 20 pA, RCF – 165 ± 14 pA, $p = 4.85 \times 10^{-4}$ (CTRL, n = 16; RCF, n = 27, Fig. 2D). The reduction of I_h amplitude was apparently not due to a down-regulation of the HCN2 protein expression as our western blotting experiments on VTA punches showed no significant difference in HCN2 level (total proteins) between RCF and Control mice (Student's *t* -test: $t = 0.6886$, df = 12, $p = 0.5042$; Supplementary Fig. 1).

Recently, Friedman and coll. (2014) showed that adult mice resilient to social defeat stress bore VTA DA neurons with up-regulated I_h current paralleled by increased K^+ currents mediated by KCNQ channels (Friedman et al., 2016). We thus asked whether in our experimental conditions (resilience to depression-like behavior associated to RCF) the observed reduction of I_h correlated with a modulation (down--regulation) of outward K^+ currents in iVTA DA neurons. To address this, we applied a family of depolarizing voltage steps to activate delayed rectifier K^+ currents and transient A-type currents (Friedman et al., 2014) but found no differences across groups (Supplementary Fig. 2), suggesting that the long-lasting neuroadaptive mechanisms activated in response to RCF might be distinct from those reported following social defeat stress. Together, our data show that RCF stably reduces R_m and I_h current in VTA DA neurons throughout adulthood.

Last, considering the relevance of DA synaptic release from VTA projections onto target neurons/areas and its impact on, for instance, depression or addiction, we asked whether also cell excitability was stably affected in adult iVTA DA neurons of the intermediate VTA following RCF. We thought that even if spontaneous firing of DA cells appeared unaffected (Figs. 1C and 2C), the high (er) frequency, evoked action potential (AP) firing could have been modulated by RCF. We explored this possibility in DA neurons of adult mice, at the same age when animal behavior was tested (see below). Indeed, we found that in response to depolarizing current injections (I_{inj}) RCF iVTA DA neurons fired APs at significantly lower frequency compared to CTRL neurons, at high stimulus intensities applied. Thus, two-way repeated measure ANOVA revealed statistical significance for *in vivo* 'treatment' (RCF vs CTRL; F (1,8) = 6.49, p = 0.034; CTRL n = 11, RCF n = 9), and a non significant interaction between *in vivo* 'treatment' and injected current (F (3,6) = 3.96, p = 0.071) besides the predicted significativity for injected current (F (3,6) = 46.51, p = 1.5 × 10-4).

The difference in firing frequency was significant at +150 and + 200 pA injected current (Bonferroni's post-hoc analysis: I_{inj} +50 pA: CTRL 3 ± 1 Hz, RCF, 1.8 ± 0.6 Hz, p = 1; I_{inj} +100 pA: CTRL, 8 ± 2 Hz and RCF, 4.6 ± 0.7 Hz, p = 0.77; I_{inj} +150 pA: CTRL, 11 ± 2 Hz and RCF, 6.6 ± 0.7 Hz, $p < 0.05$; I_{inj} +200 pA, CTRL, 13 ± 2 Hz and RCF, 8.2 ± 0.6 Hz, $p < 0.05$; Fig. 2E). These results indicate that besides Ih reduction and Rm drop, RCF caused the decrease of evoked firing in adult iVTA DA neurons; such electrophysiological alterations are then possibly linked to the resilient behavior shown by adult RCF mice (Di Segni et al., 2017, 2019).

3.3. *Intra-VTA infusion of lamotrigine potentiates I_h in DA neurons and counteracts the pro-resilient RCF behavioral phenotype in female mice*

If the reduction of I_h current induced by early experience is at least partially responsible for the lesser passive coping and increased saccharin preference that we previously reported in RCF female mice (Di Segni et al., 2017, 2019), then a pharmacological interference targeted to HCN channel functions *in vivo* should revert the behavioral and electrophysiological phenotypes observed.

To test this hypothesis, firstly we aimed at potentiating the I_h current in iVTA DA neurons of RCF adult female animals by repeated, stereological intra-VTA infusion of lamotrigine (LTG), a voltage-gated sodium channel blocker used for its antiepileptic effects and recently found to also serve as HCN channel enhancer (Friedman et al., 2014; Huang et al., 2016).

In line with our hypothesis, RCF animals with repeated intra-VTA infusion of LTG (RCF-LTG mice) showed increased immobility behavior compared to control group (RCF-Veh) in both FST ($p < 0.05$, *t* -test = −2.4, 8 and 6 mice for RCF-Veh and RCF-LTG groups, respectively) and TST ($p < 0.001$, *t* -test = −5.04, 5 and 6 mice for RCF-Veh and RCF-LTG). Moreover, two-way ANOVA performed on percentage of saccharin intake revealed a significant intake effect ($F_{(1,9)} = 31.07$; $p < 0.001$; 5 and 6 mice for RCF-Veh and RCF-LTG) and a significant intake x pharmacological manipulation interaction ($F_{(1,9)} = 10.77$; $p < 0.01$; Fig. 3A). Of note, *post-hoc* analysis unveiled that, even if both RCF-Veh ($p < 0.001$) and RCF-LTG ($p < 0.01$) groups showed a significant preference for saccharin, RCF-Veh had higher percentage of saccharin intake than RCF-LTG ($p < 0.01$; Fig. 3A). Thus, intra-VTA LTG infusion succeeded in counteracting the pro-resilient to depression-like phenotype observed in RCF female mice.

Considering that LTG may exert different effects on distinct ion channels (including voltage-gated Na^+ channels), we wanted to verify at

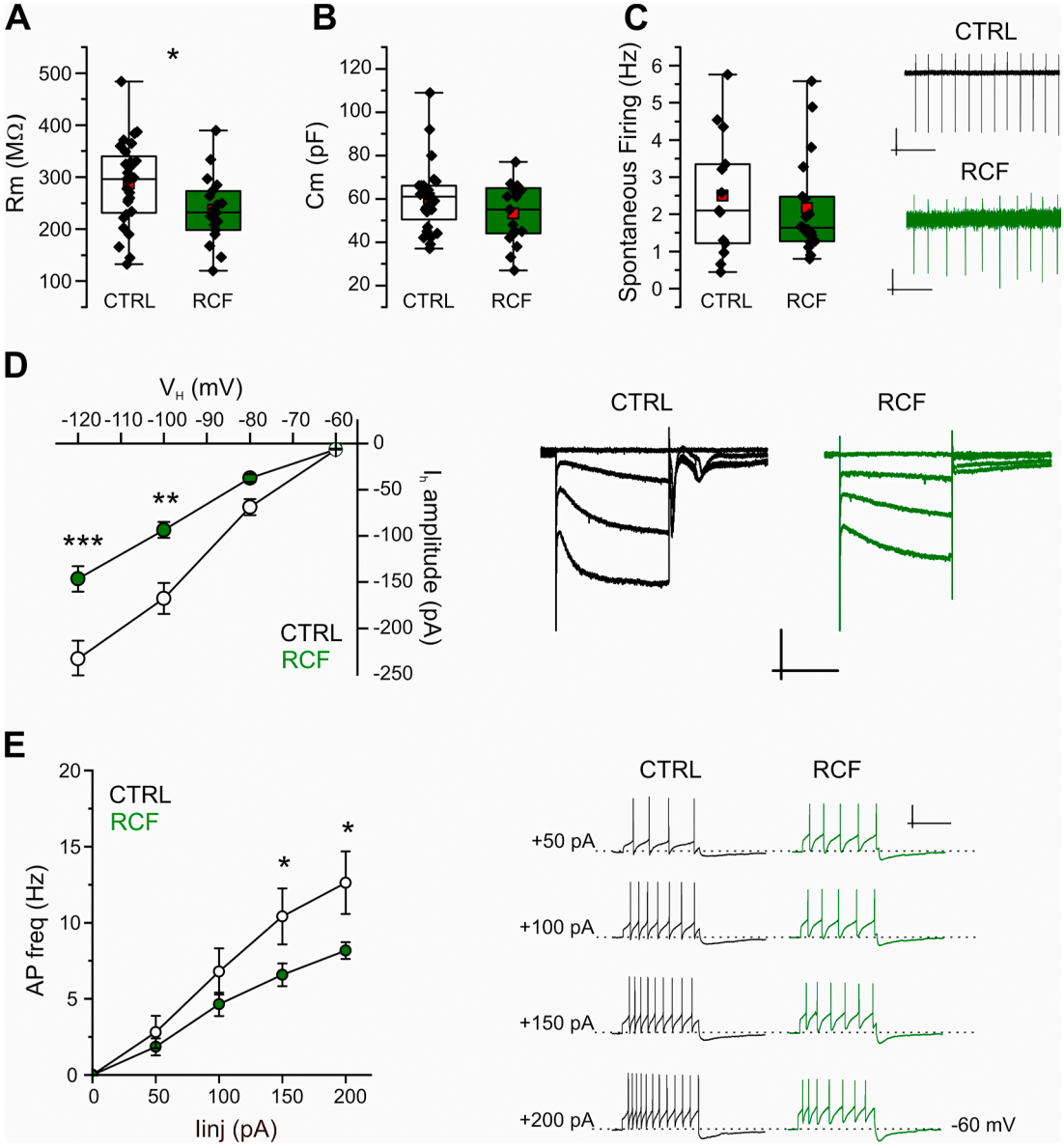

Fig. 2. Adult RCF mice show altered R_m, I_h and evoked AP firing in DA neurons of iVTA *A*, Membrane resistance (R_m) of DA neurons in the iVTA from adult RCF mice (P60) is significantly reduced compared to Controls: CTRL 287 ± 15 MΩ and RCF 237 ± 15 MΩ (n = 28 and 19, respectively; Student's *t*-test, t = 2.38, df = 43.86, $*p < 0.05$). *B*, Similar membrane capacitance across conditions: CTRL 60 ± 3 pF and RCF 53 ± 3 pF (28 and 19 neurons, respectively; t = 1.63, df = 42.16, $p = 0.11$). *C*, Similar AP spontaneous firing frequency between Control and RCF mice: CTRL 2.5 ± 0.4 Hz and RCF 2.1 ± 0.3 Hz (13 and 19 cells, respectively; t = 0.62, df = 22.02, $p = 0.54$; inset: typical cell-attached recordings). Scale bars: upper 30 pA, 1 s; lower 5 pA, 1 s. *D*, to the left: I–V curves depicting significant reduction of I_h amplitude in VTA DA neurons from RCF mice. In details, the two-way repeated measure ANOVA analysis returned: for '*in vivo* treatment' (RCF vs CTR) $F_{(1,15)} = 10.49$, $**p = 0.0055$; for membrane potential (V_H), $F_{(3,13)} = 73.49$, $***p = 2.08 \times 10^{-8}$; and for the interaction treatment x membrane potential $F_{(3,13)} = 3.016$, $*p = 0.0489$. The Bonferroni's *post-hoc* analysis returned: at V_H – 60 mV, CTRL – 6.8 ± 0.7 pA, RCF – 6 ± 1 pA, $p = 1$; at V_H – 80 mV, CTRL – 69 ± 9 pA, RCF – 42 ± 5 pA, $p = 1$; at V_H – 100 mV, CTRL – 168 ± 17 pA, RCF – 104 ± 9 pA, $**p = 0.0015$; at V_H – 120 mV, CTRL – 233 ± 20 pA, RCF – 165 ± 14 pA, $***p = 4.85 \times 10^{-4}$ (CTRL, n = 16; RCF, n = 27). To the right, example I_h current traces (four superimposed consecutive sweeps). Scale bars: 200 pA, 0.5 s. *E*, frequency – injected current amplitude (*f* – I) average relationship (left) for evoked APs in adult CTRL or RCF neurons depicting significantly reduced ability to elicit APs in RCF mice. In details: for *in vivo* treatment $F_{(1,8)} = 6.49$, $*p = 0.034$; interaction treatment x injected current $F_{(3,6)} = 3.96$, $p = 0.071$; for injected current $F_{(3,6)} = 46.51$, $***p = 1.5 \times 10^{-4}$ (two-way repeated measure ANOVA). The Bonferroni's *post-hoc* analysis returned: with I_{inj} +50 pA: CTRL 3 ± 1 Hz, RCF, 1.8 ± 0.6 Hz, $p = 1$; I_{inj} +100 pA: CTRL, 8 ± 2 Hz and RCF, 4.6 ± 0.7 Hz, $p = 0.77$; I_{inj} +150 pA: CTRL, 11 ± 2 Hz and RCF, 6.6 ± 0.7 Hz, $*p < 0.05$; I_{inj} +200 pA, CTRL, 13 ± 2 Hz and RCF, 8.2 ± 0.6 Hz, $*p < 0.05$. To the right, typical current-clamp recordings showing evoked firing. Scale bars: 30 mV, 1 s.

the cellular level that indeed *in vivo* repeated application of the HCN enhancer could potentiate the I_h current in iVTA DA neurons of infused animals without affecting other functional properties. Thus, we investigated sub- and supra-threshold properties of iVTA DA neurons of the intermediate VTA in brain slices from RCF-LTG and RCF-Veh adult mice and confirmed that whilst DA neurons were unaffected by stereological infusions in both passive and active properties (Table 1), the I_h current density recorded in response to hyperpolarizing voltage steps from RCF-LTG neurons was significantly larger compared to RCF-Veh. Thus, the two-way ANOVA with repeated measures on the I–V relationships returned for I_h current density in RCF-Veh and RCF-LTG mice $F_{(1,29)} = 4.84$ and $p = 0.0359$ (13 and 18 neurons, respectively), with weak interaction between I_h current density and V_H ($p = 0.0621$) and predictably significant effect of V_H ($p < 0.0001$; Fig. 3B). No difference was

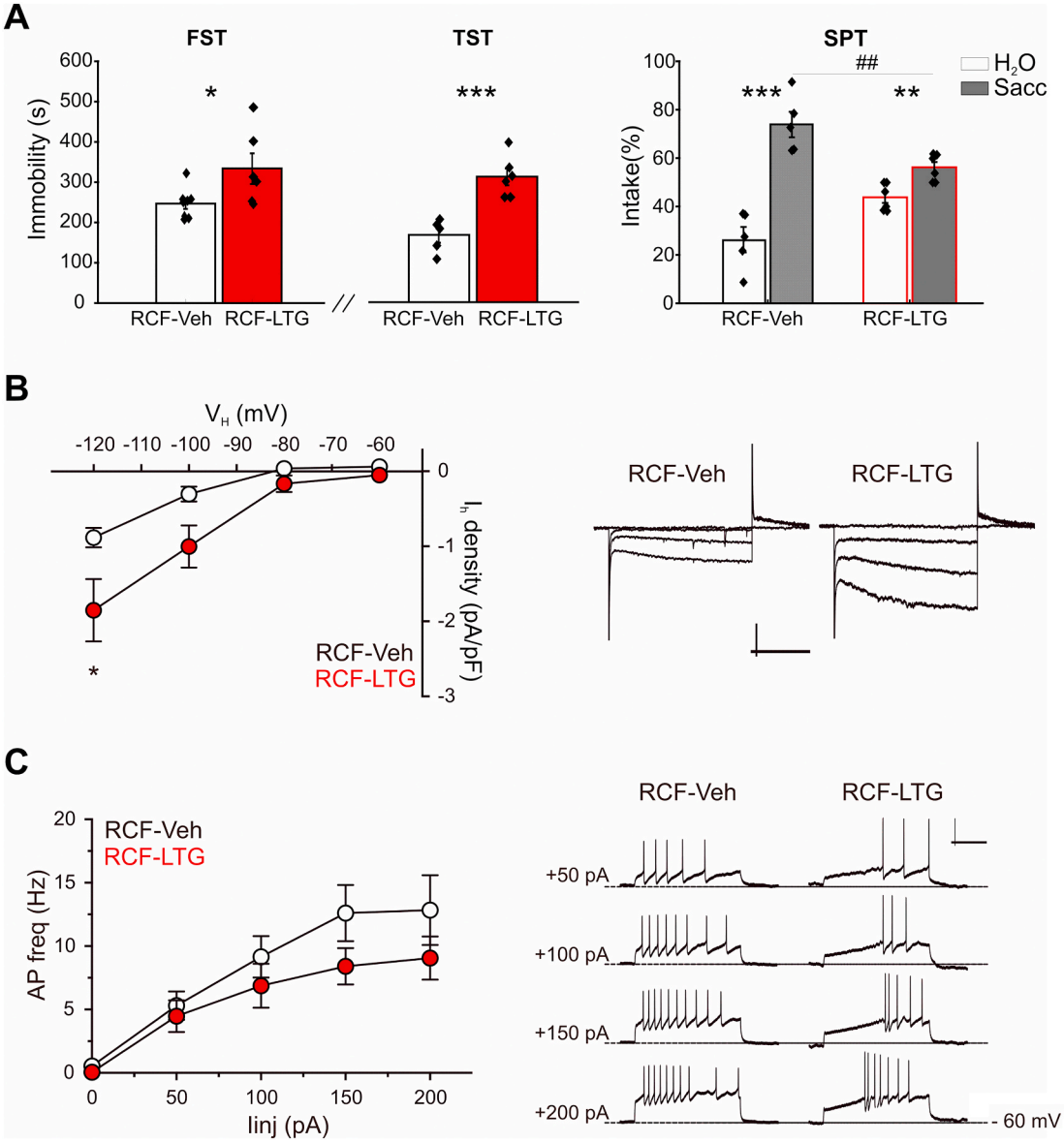

Fig. 3. Adult RCF mice intra-VTA infused with Lamotrigine rescue Control behavior and show potentiated I_h current *A*, pooled data for Forced Swim Test (FST; left), Tail Suspension Test (TST; middle) and Saccharin Preference Test (SPT, right). RCF mice intra-VTA infused with Lamotrigine (RCF-LTG) show increased immobility behavior in both FST (*$p < 0.05$, *t* -test = −2.4, 8 RCF-Veh and 6 RCF-LTG mice) and TST (***$p < 0.001$, *t* -test = −5.04, 5 RCF-Veh and 6 RCF-LTG mice) as well as reduced percentage of saccharin intake in comparison with Vehicle-treated animals (RCF-Veh; *$p < 0.01$). *B*, I–V curves depicting significant potentiation of I_h current density in DA neurons in the iVTA from RCF-LTG mice compared to RCF-Veh: two-way ANOVA with repeated measures showed statistical difference for 'treatment' (i.e. LTG infusion; *$p = 0.0359$), weak interaction between I_h amplitude and V_H ($p = 0.0621$) and predictably significant effect of V_H (***$p < 0.0001$). *Post-hoc* Bonferroni's multiple comparisons test showed that I_h current density recorded at V_H – 120 mV was significantly larger in RCF-LTG neurons (*$p < 0.05$; 13 RCF-Veh and 18 RCF-LTG neurons). To the right, typical I_h currents. Scale bars: 100 pA, 0.3 s. *C*, *f* – I relationships (left) and typical current-clamp recordings (right) depicting lack of difference in frequency of APs evoked in RCF-LTG and RCF-Veh neurons: two-way ANOVA with repeated measures showed no difference for 'treatment' (i.e. LTG infusion; $p = 0.2190$) at the I_{inj} shown (13 RCF-Veh and 17 RCF-LTG neurons). Note the increased latency of the first evoked spike in RCF-LTG neurons. Scale bars: 30 mV, 0.3 s.

Table 1
Sub- and supra-threshold properties of DA neurons of the intermediate VTA are unaffected by intra-VTA infusion of LTG in RCF adult females.

	RP (mV)	τ_{memb} (ms)	R_{in} (MΩ)	C_m (pF)	SponAP (Hz)	Rheo (pA)	V_{thre} (mV)
RCF-Veh	*−52 ± 2 (14)*	*1.2 ± 0.2 (13)*	*279 ± 32 (14)*	*45 ± 4 (3)*	*1.9 ± 0.5 (10)*	*108 ± 20 (10)*	*−35 ± 8 (11)*
RCF-LTG	*−51 ± 2 (18)*	*1.14 ± 0.07 (18)*	*226 ± 18 (18)*	*44 ± 3 (18)*	*2.2 ± 0.5 (17)*	*177 ± 28 (11)*	*−40 ± 2 (11)*
p value	*0.5435*[a]	*0.6826*[a]	*0.1586*[a]	*0.7409*[a]	*0.9586*[b]	*0.0625*[a]	*0.6407*[b]

The table summarizes average ± SEM values (cells analyzed are in brackets) for membrane approximate 'resting' potential (RP), time constant (τ_{memb}), input resistance (R_{in}), capacitance (C_m), spontaneous action potential firing (SponAP, in whole-cell), rheobase (Rheo) and AP threshold (V_{thre}). Bottom, relevant *p* values.
[a] Unpaired *t*-test with Welch's correction.
[b] Mann Whitney test.

found when comparing the evoked firing of RCF-LTG and RCF-Veh neurons (two-way ANOVA with repeated measures on the *f* - I relationships: $F_{(1,28)} = 1.581$; $p = 0.2190$, 13 and 17 neurons from respectively RCF-Veh and RCF-LTG mice; interaction between firing frequency and I_{inj}, $p = 0.2445$, with predictably significant effect of I_{inj}, $p < 0.0001$; Fig. 3C). Of note, the latency of the first evoked AP (measured from the beginning of the injected current step) was significantly larger in neurons from LTG-infused compared to Vehicle-infused animals (RCF-Veh 174 ± 38 ms, 13 neurons *vs* RCF-LTG 343 ± 67 ms, 17 neurons; $p = 0.037$ by unpaired *t*-test with Welch correction; Fig. 3 C). This effect, most probably due to the blocking activity of LTG on voltage-gated Na^+ channels, further confirmed the efficacy of intra-VTA infused LTG *ex-vivo*.

No effects were found both at the behavioral and the electrophysiological level when investigating the consequences of intra-VTA LTG infusion in naïve female mice (that is, animals which did not experience RCF).

Thus, at the behavioral level intra-VTA infusion of LTG in naïve mice

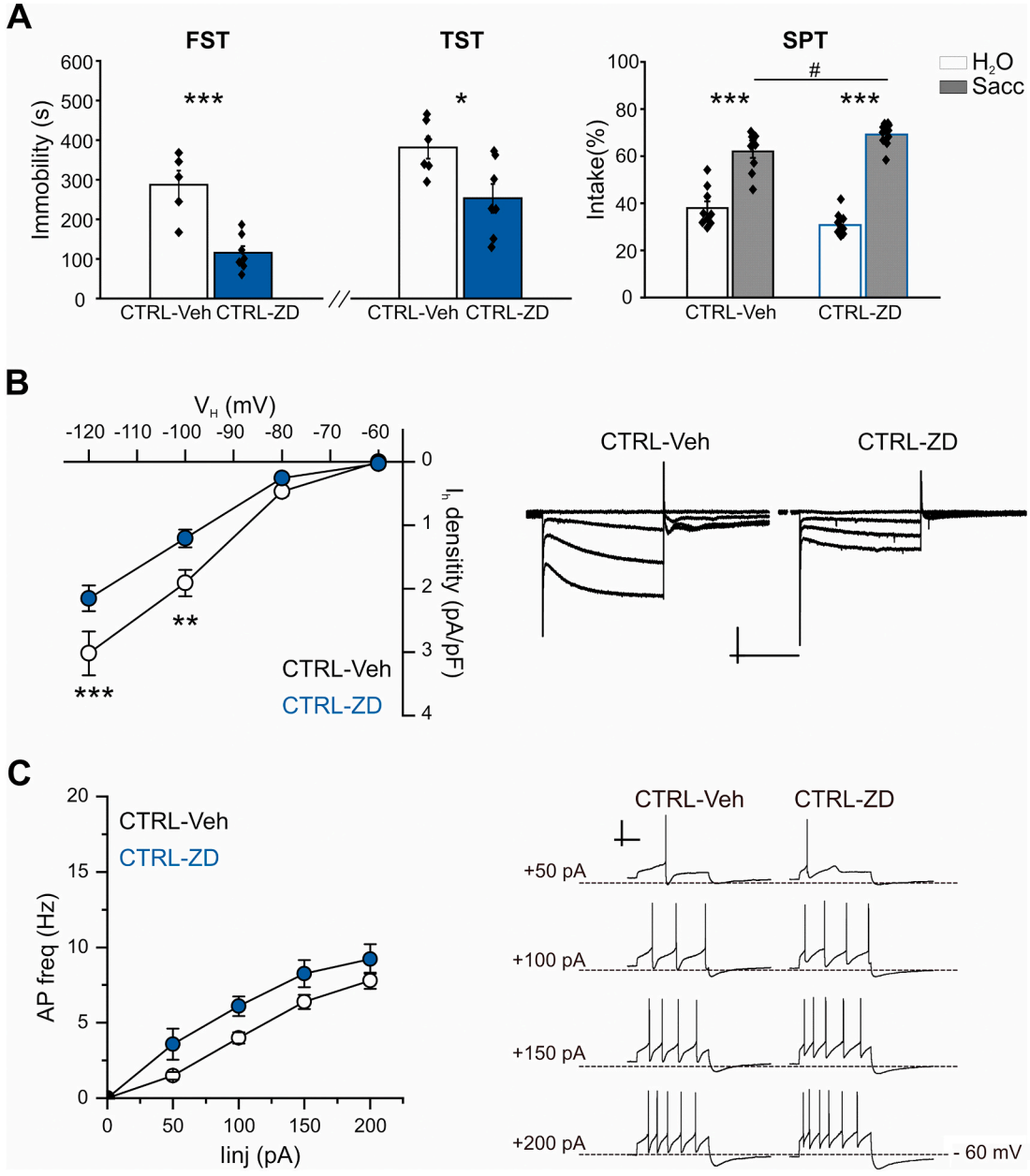

Fig. 4. Adult Control mice intra-VTA infused with ZD7288 show RCF behavior and reduced I_h current *A*, pooled data for Forced Swim Test (FST; left), Tail Suspension Test (TST; middle) and Saccharin Preference Test (SPT, right). Control mice intra-VTA infused with ZD7288 (CTRL-ZD) show reduced immobility behavior in both FST (***$p < 0.001$, *t* -test = 4.69, 7 CTRL-ZD and 6 CTRL-Veh mice) and TST (*$p < 0.05$, *t* -test = 2.7, 7 CTRL-ZD and 6 CTRL-Veh) as well as increased percentage of saccharin intake in comparison with Vehicle-treated animals (CTRL-Veh mice; $p < 0.05$). *B*, to the left, I–V curves depicting significant reduction of I_h current density in DA neurons in the iVTA from CTRL-ZD mice compared to CTRL-Veh. Two-way repeated measures ANOVA: *in vivo* treatment, $F_{(1,31)} = 8.58$, **$p = 0.0063$; *in vivo* treatment x membrane potential, $F_{(3,29)} = 7.09$, **$p = 0.0010$; membrane potential, $F_{(3,29)} = 48.21$, ***$p = 2.17 \times 10^{-11}$. For CTRL-Veh vs CTRL-ZD with Bonferroni's *post-hoc* analysis: at V_h −60 mV, CTRL-Veh 0 ± 1 pA, CTRL-ZD – 2 ± 1 pA, $p = 1$; at V_h −80 mV, CTRL-Veh – 37 ± 5 pA, CTRL-ZD – 17 ± 3 pA, $p = 1$; at V_h −100 mV, CTRL-Veh – 138 ± 15 pA, CTRL-ZD – 76 ± 10 pA, **$p = 0.0029$; at V_h – 120 mV, CTRL-Veh – 204 ± 23 pA, CTRL-ZD – 137 ± 15 pA, ***$p = 8.12 \times 10^{-4}$ (CTRL-Veh, n = 40; CTRL-ZD, n = 32). To the right, example I_h currents. Scale bars: 200 pA, 0.5 s. *C*, *f* – I relationships (left) and typical current-clamp recordings (right) depicting lack of difference in frequency of APs evoked in CTRL-ZD and CTRL-Veh neurons, as revealed by two-way repeated measures ANOVA: treatment, $F_{(1,28)} = 3.4$, $p = 0.075$; treatment x I_{Inj} $F_{(3,26)} = 0.099$, $p = 0.95$; (CTRL-Veh n = 39, CTRL-ZD n = 30). Scale bars: 30 mV, 1 s.

(CTRL-LTG mice) does not induce significant differences in immobility between CTRL-LTG and CTRL-Veh in both FST (ns, t -test = 1.8; n = 5 for group) and TST (ns, t -test = 0.6; 5 for group). Two-way ANOVA performed on percentage of saccharin intake revealed a significant intake effect ($F_{(1,8)} = 21.34$; $p < 0.01$; n = 5 for group) but no significant intake x pharmacological manipulation interaction ($F_{(1,8)} = 0.107$; ns; Supplementary Fig. 3).

In line with these findings, we found no effect on both the I–V relationship (two-way ANOVA with repeated measures: $F_{(1,12)} = 0.3304$, $p = 0.5760$; 7 CTRL-Veh and 7 CTRL-LTG cells) and the *f* – I relationship of evoked firing (two-way ANOVA with repeated measures: $F_{(1,10)} = 2.150$, $p = 0.1733$; 7 CTRL-Veh and 5 CTRL-LTG cells) in naïve mice (Supplementary Fig. 3).

3.4. Intra-VTA infusion of ZD7288 reduces I_h in DA neurons and recapitulates the pro-resilient behavioral phenotype of RCF female mice

To further support our hypothesis of a role for I_h current in the resilient behavior of RCF female mice, we performed stereological intra-VTA infusion of ZD7288 (ZD), a selective blocker of HCN channels (Cao et al., 2010; Yang et al., 2016) to mimic RCF phenotype both *in vivo* and *ex vivo* in Control adult animals.

Indeed repeated intra-VTA infusion of ZD (CTRL-ZD mice) reduced immobility compared to Veh mice (CTRL-Veh) during both FST ($p < 0.001$, *t* -test = 4.69, 7 CTRL-ZD and 6 CTRL-Veh mice) and TST ($p < 0.05$, *t* -test = 2.7, 7 CTRL-ZD and 6 CTRL-Veh mice; Fig. 4A). Moreover, two-way ANOVA performed on percentage of saccharin intake revealed both a significant intake effect ($F_{(1,17)} = 102{,}65$; $p < 0.001$, 10 CTRL-ZD and 9 CTRL-Veh mice) and a significant intake x pharmacological manipulation interaction ($F_{(1,17)} = 5.45$; $p < 0.05$). Again, *post-hoc* analysis showed that, even if both CTRL-Veh and CTRL-ZD groups had a significant preference for saccharin (both $p < 0.001$), CTRL-ZD mice showed higher saccharin preference compared to CTRL-Veh ($p < 0.05$; Fig. 4A). Thus, blocking HCN channels in the VTA of Control animals recapitulates the resilience to depression-like behavior seen in RCF females.

To confirm that chronic *in vivo* intra-VTA administration of ZD indeed reduced I_h current, we performed patch-clamp recordings from iVTA DA neurons and found that ZD application did not alter R_m (CTRL-Veh, 353 ± 24 MΩ, n = 39, CTRL-ZD 399 ± 31 MΩ, n = 34, Student's *t*-test = −1.17, df = 65.18, $p = 0.25$) nor spontaneous AP firing (CTRL-Veh, 2.3 ± 0.2 Hz and CTRL-ZD, 2.9 ± 0.5 Hz, n = 31 and 17, respectively, Student's *t*-test = 1.27, df = 24.62, $p = 0.21$) with only a slight decrease of C_m (CTRL-Veh, 71 ± 3 pF and CTRL-ZD, 61 ± 3 pF, n = 39 and 34, respectively, Student's *t*-test = 2.28, df = 70.90, $p < 0.05$). Instead, as expected, I_h amplitude was significantly reduced in iVTA DA neurons from ZD-injected mice, and this was independent on the smaller cell size caused by ZD. Indeed, I_h current density from CTRL-ZD neurons was significantly reduced compared to CTRL-Veh (two-way ANOVA with repeated measures on the I–V relationships: $F_{(1,31)} = 8.58$; $p = 0.0063$, 40 and 32 neurons for CTRL-Veh and CTRL-ZD mice; Fig. 4B). Similar to what found after LTG infusion on RCF mice, frequency of evoked firing remained unaltered in DA neurons of the iVTA after site-specific administration of ZD (two-way repeated measures ANOVA: treatment $F_{(1,28)} = 3.40$, $p = 0.075$, CTRL-Veh, n = 39, CTRL-ZD, n = 30, Fig. 4C).

Together, our results indicate that indeed *in vivo* stereological, intra-VTA infusion of pharmacological agents able to either potentiate (LTG) or block (ZD7288) HCN channels and I_h current can, respectively, revert the resilient phenotype in adult RCF mice or confer 'resilience' to Control animals. This observation strongly supports the hypothesis of a role for the I_h current of VTA DA neurons in the causative link between early life adversity (RCF) exposure and adult resilience to depression-like behaviors.

4. Discussion

Resilience has been defined as 'the process of adapting well in the face of adversity' (Charney, 2004) and has been specifically linked to neuroadaptations within the VTA-NAc circuit, known to play a relevant role in reward- and emotion-related behaviors (Nestler and Carlezon, 2006). We have previously demonstrated that exposure to RCF increases resilience to depression-like behavior in adult female C57 mice (Di Segni et al., 2016, 2017) while increases anhedonia and depression-related behaviors in C57 males (2019).

Aim of the present work was to investigate the consequence(s) of RCF manipulation on the functional properties of DA neurons of the iVTA, which could underlie the pro-resilient behavioral phenotype of adult RCF female mice.

We found that RCF affected the same functional parameters of VTA DA neurons as other *in vivo* stress manipulations, but in a unique way: early stress reduced the hyperpolarization-activated I_h current and the evoked neuronal firing in both young P16-22) and adult (P60-70) RCF animals compared to controls, leaving the spontaneous neuronal firing unaffected. Lower membrane resistance of the recorded neurons accompanied these modifications at both ages. Although functional and morphological effects of early stress within the VTA have been recently reported (Authement et al., 2015; Shepard et al., 2020; Spyrka et al., 2020; Masrouri et al., 2020), this is, to our knowledge, the first evidence showing how pro-resilience behavior induced by early events is linked to a long-lasting reduction of I_h current (and excitability) of VTA DA neurons. This interpretation is strongly supported by our results from *in vivo* pharmacological treatments.

4.1. RCF reduces membrane resistance in VTA DA neurons

The first evidence evicted from our current-clamp analysis of DA neurons of young and adult female mice demonstrated that RCF manipulation stably reduces, since early post-natal life and well into adulthood, the membrane resistance of iVTA DA neurons. The sensitivity of this phenomenon to intracellular Cs^+, a broad-spectrum blocker for K^+ channels, suggests the steady activation of a K^+ conductance. Recently, Friedman and coll. (2014; 2016) showed that the K^+ currents potentiated in VTA DA neurons of resilient mice (exposed to adult stress) were mediated by delayed rectifier (DR) K^+ channels. At odd with their findings, we observed no modulations of DR K^+ channels in adult RCF mice. However, different types of K^+ channels are involved with behavioral resilience. For example, the up-regulation of Kv3.1 channels in DA gyrus neurons can induce resilience to depression in mice (Medrihan et al., 2020); or, the over-expression of an inwardly rectifying K^+ channel (Kir2.1) in VTA DA neurons can promote resilience in social defeated mice (Krishnan et al., 2007). At this stage, further investigation is needed to clarify which subtype of K^+ channels, if any, is modulated by RCF.

Besides active, intrinsic properties of neuronal membranes, many other factors can strongly influence membrane resistance like, for instance, synaptic activity in general as well as dendritic complexity (Al-muhtasib et al., 2018). The latter neuronal features are characterized by strong plasticity, particularly during the early stages of development of the nervous system. With regards to neuroadaptive cellular modifications influencing behavioral phenotypes, it has been reported that the dendritic harborization of limbic cortical neurons undergoes opposite changes, depending on whether the mouse phenotype will be susceptible or resilient to depression (Lguensat et al., 2019). VTA DA neurons are no exception to this, as it has been recently reported that maternal separation causes dendritic spine heads modifications (Spyrka et al., 2020). Even if we didn't address details of synaptic transmission to the level of spine analysis here, we found no functional differences between RCF and CTRLs relevant to excitatory transmission, suggesting that our manipulation does not interfere with the development of the glutamatergic projections onto VTA DA neurons.

4.2. RCF reduces I_h current and evoked firing in VTA DA neurons

A functional feature of neuronal membranes modified in stress-resilient models is the I_h current, which undergoes up- or down-regulation depending on neuronal type, brain area and/or stress protocol adopted. Thus, for instance, I_h current appeared increased in VTA DA neurons of resilient rodents subject to adult stress protocol (Friedman et al., 2014), but was reduced in animals subjected to chronic mild stress (Zhong et al., 2018). Further, I_h was found to be down-regulated in the principal neurons of the basolateral amygdala of stress-resilient rats (Villarroel et al., 2018) and in the dorsal CA1 region, where its reduction was sufficient to provide resilience to chronic unpredictable stress in rats (Kim and Johnson, 2018). We add to this scenario by reporting for the first time that the I_h current of DA neurons in the iVTA of resilient female mice exposed to early life adversity is significantly reduced. This finding is not conflicting with the potentiation of I_h (and K^+) currents found for the same neurons following adulthood stress-exposure (Friedman et al., 2014), as it's well conceivable that the degree of neuronal maturation at the time of stress exposure as well as the stress protocol adopted may dictate the direction of I_h modulation.

To some surprise, the modulation of the I_h amplitude reported here is seemingly independent of the expression of HCN2 protein in the VTA (western blotting). However, different caveats should be considered with regards to this set of data; firstly, the HCN2 surface/intracellular ratio has been not quantified here, a factor limiting our estimate of HCN2 functional proteins in neuronal membranes (Santos-Vera et al., 2019). Secondly, the expression of the HCN2 subunit was estimated from 'total' VTA punches, inevitably including every cell type present in the tissue sample analyzed, not only DA neurons. For instance, Margolis et al. (2012) showed that within the VTA HCN2 channels are also expressed in GABA-ergic neurons. Thus, finer (possibly cell-specific) isolation and detection methods will be required to investigate in deep the possible modifications induced by the RCF manipulation on HCN2 (or other) channel subunits in DA neurons. Last, yet importantly, the reduction of I_h amplitude might well depend on functional, rather than 'structural', modulation(s) of the current.

Different works on animals bearing resilient response to adult stress showed that VTA neurons had unaltered spontaneous firing, recorded either *in vitro* or *in vivo* (Krishnan et al., 2007; Cao et al., 2010; Chaudhury et al., 2013; Isingrini et al., 2016). In line with these findings, we also observed unaltered spontaneous firing in iVTA DA neurons of resilient RCF mice, both during adolescence (P16-22) and in adulthood (P60).

Why do we observe reduced evoked firing in RCF adults? The potentiation of DR K+currents in resilient mice reported by Friedman and coll. (2014) represents the homeostatic response to the hyper-excitability of VTA-NAc neurons; this is due to the increased stimulation of their α1 and β3 adrenergic receptors activated in the Locus Coeruleus-VTA pathway (Zhang et al., 2019). As a consequence of this strong homeostatic plasticity, resilient mice showed depressed firing. Here, the involvement of DR K^+ channels can be excluded; yet, the Cs-sensitivity of the lower membrane resistance observed suggests that some K^+ conductance might mediate membrane shunt of evoked firing - an open question worth further investigations.

4.3. Pharmacological modulation of VTA DA neurons I_h current is able to affect behavioral phenotype

Based on our results, we hypothesized that reduced I_h current could be responsible for the resilient behavioral phenotype induced by early life adversity exposure in female mice. To test this hypothesis, we adopted an *in vivo* pharmacological approach and locally infused either LTG (to potentiate I_h current; Friedman et al., 2014) in RCF animals or ZD (a HCN channel blocker; Cao et al., 2010; Zhong et al., 2018) in CTRL mice. For both treatments, patch-clamp recording from VTA DA neurons confirmed that the infused drug efficaciously reached the target area; in line with this, we found that LTG and ZD could, respectively, increase passive coping in FST and TST while reducing saccharine preference in RCF animals and recapitulate the RCF resilient behavior in CTRL animals (reduced passive coping behavior and increased saccharine preference). The finding that the pharmacological modulation of HCN channels expressed in the VTA of adult mice can either revert (LTG) or mimic (ZD) the behavioral phenotype induced by RCF is relevant and identifies the I_h current in iVTA DA neurons as a contributor, to say the least, in determining the adult coping strategy shaped by early experience.

5. Conclusions

Stress is commonly used to induce depression-like behavior in animals (Slattery and Cryan, 2017; Chang and Grace, 2014; Rincón-Cortés and Grace, 2017). In resilience, effective coping strategies will allow to manage stress and return to homeostasis; depression, instead, will manifest when these strategies are inadequate or inappropriate (Gururajan et al., 2019). The modulation of VTA DA neurons has been linked to both these responses (Friedman et al., 2014, 2016; Cao et al., 2010; Zhong et al., 2018; Kaufling 2019; Luo et al., 2019; Tan et al., 2020; Zhang et al., 2019; Cheng et al., 2019; Tye et al., 2013). Here, by implementing a multi-disciplinary approach, we add to the current knowledge in the field and report that female C57 mice subjected to early life adversity and bearing a pro-resilient phenotype in adult age show reduced I_h current amplitude and evoked firing in DA neurons of the iVTA. *In vivo*, targeted pharmacological manipulation of I_h –mediating channels did revert the pro-resilient phenotype in adult mice exposed to early life adversity (using the HCN enhancer LTG), or mimic the RCF phenotype in adult CTRL animals (using the HCN blocker ZD). Overall, our data demonstrate that early experiences impact DA neurons of the VTA since immediately post-natal life well into adulthood by altering their I_h current.

Funding

This research was supported by Ministero della Ricerca Scientifica e Tecnologica (FIRB 2010; RBFR10RZ0N_001); Ateneo 2018 (RP118164336EF3FD); Ateneo 2020 (RM120172B7A3A801), University Sapienza, Rome, Italy.

CRediT authorship contribution statement

Sebastian Luca D'Addario: Conceptualization, Investigation, Formal analysis. **Matteo Di Segni:** Conceptualization, Investigation, Formal analysis. **Ada Ledonne:** Conceptualization, Investigation, Formal analysis. **Rosamaria Piscitelli:** Investigation, Formal analysis. **Lucy Babicola:** Investigation, Formal analysis. **Alessandro Martini:** Investigation, Formal analysis. **Elena Spoleti:** Investigation, Formal analysis. **Camilla Mancini:** Investigation, Formal analysis. **Donald Ielpo:** Investigation, Formal analysis. **Francesca R. D'Amato:** Conceptualization, Writing – review & editing. **Diego Andolina:** Conceptualization, Methodology. **Davide Ragozzino:** Writing – review & editing. **Nicola B. Mercuri:** Writing – review & editing. **Carlo Cifani:** Methodology, Writing – review & editing. **Massimiliano Renzi:** Investigation, Formal analysis, Writing – review & editing. **Ezia Guatteo:** Conceptualization, Methodology, Formal analysis, Writing – original draft, Supervision. **Rossella Ventura:** Conceptualization, Methodology, Writing – original draft, Supervision, Funding acquisition.

Declarations of competing interest

None.

Data availability

Data will be made available on request.

Acknowledgement

We thank the Zardi-Gori Foundation for Lucy Babicola research fellowship.

Appendix A. Supplementary data

Supplementary data to this article can be found online at https://doi.org/10.1016/j.ynstr.2021.100324.

References

Al-muhtasib, N., Forcelli, P.A., Vicini, S., 2018. Differential electrophysiological properties of D1 and D2 spiny projection neurons in the mouse nucleus accumbens core. Physiological reports 6, e13784.
American Psychiatric Association, 2013. Diagnostic and Statistical Manual of Mental Disorders, fifth ed. Washington, DC.
Andersen, S.L., 2015. Exposure to early adversity: points of cross-species translation that can lead to improved understanding of depression. Dev. Psychopathol. 27, 477–491.
Andolina, D., Di Segni, M., Accoto, A., Iacono, L.L., Borreca, A., Ielpo, D., Berretta, N., Perlas, E., Puglisi-Allegra, S., Ventura, R., 2018. MicroRNA-34 contributes to the stress-related behavior and affects 5-HT prefrontal/GABA amygdalar system through regulation of corticotropin-releasing factor receptor 1. Mol. Neurobiol. 55, 7401–7412.
Authement, M.E., Kodangattil, J.N., Gouty, S., Rusnak, M., Symes, A.J., Cox, B.M., Nugent, F.S., 2015. Histone deacetylase inhibition rescues maternal deprivation-induced GABAergic metaplasticity through restoration of AKAP signaling. Neuron 86, 1240–1252.
Bean, B.P., 2007. The action potential in mammalian central neurons. Nat. Rev. Neurosci. 8, 451–465.
Bellone, C., Mameli, M., Lüscher, C., 2011. In utero exposure to cocaine delays postnatal synaptic maturation of glutamatergic transmission in the VTA. Nat. Neurosci. 14, 1439–1446.
Belsky, J., Newman, D.A., Widaman, K.F., Rodkin, P., Pluess, M., Fraley, R.C., Berry, D., Helm, J.L., Roisman, G.I., 2015. Differential susceptibility to effects of maternal sensitivity? A study of candidate plasticity genes. Dev. Psychopathol. 27, 725–746.
Belsky, J., Pluess, M., 2009. Beyond diathesis stress: differential susceptibility to environmental influences. Psychol. Bull. 135, 885–908.
Belsky, J., Pluess, M., 2013. Beyond risk, resilience, and dysregulation: phenotypic plasticity and human development. Dev. Psychopathol. 25, 1243–1261.
Belujon, P., Grace, A.A., 2017. Dopamine system dysregulation in major depressive disorders. Int. J. Neuropsychopharmacol. 20 (12), 1036–1046.
Belujon, P., Grace, A.A., 2014. Restoring mood balance in depression: ketamine reverses deficit in dopamine-dependent synaptic plasticity. Biol. Psychiatr. 76, 927–936.
Blood, A.J., Iosifescu, D.V., Makris, N., Perlis, R.H., Kennedy, D.N., Dougherty, D.D., Kim, B.W., Lee, M.J., Wu, S., Lee, S., Calhoun, J., Hodge, S.M., Fava, M., Rosen, B.R., Smoller, J.W., Gasic, G.P., Breiter, H.C., 2010. A. Phenotype Genotype Project on, D. Mood, Microstructural abnormalities in subcortical reward circuitry of subjects with major depressive disorder. PloS One 5, e13945.
Brake, W.G., Zhang, T.Y., Diorio, J., Meaney, M.J., Gratton, A., 2004. Influence of early postnatal rearing conditions on mesocorticolimbic dopamine and behavioural responses to psychostimulants and stressors in adult rats. Eur. J. Neurosci. 19, 1863–1874.
Cao, J.L., Covington 3rd, H.E., Friedman, A.K., Wilkinson, M.B., Walsh, J.J., Cooper, D. C., Nestler, E.J., Han, M.H., 2010. Mesolimbic dopamine neurons in the brain reward circuit mediate susceptibility to social defeat and antidepressant action. J. Neurosci. 30, 16453–16458.
Carbone, C., Costa, A., Provensi, G., Mannaioni, G., Masi, A., 2017. The hyperpolarization-activated current determines synaptic excitability, calcium activity and specific viability of substantia nigra dopaminergic neurons. Front. Cell. Neurosci. 11, 187.
Caspi, A., Hariri, A.R., Holmes, A., Uher, R., Moffitt, T.E., 2010. Genetic sensitivity to the environment: the case of the serotonin transporter gene and its implications for studying complex diseases and traits. Am. J. Psychiatr. 167, 509–527.
Chang, C.H., Grace, A.A., 2014. Amygdala-ventral pallidum pathway decreases dopamine activity after chronic mild stress in rats. Biol. Psychiatr. 76, 223–230.
Charney, D.S., 2004. Psychobiological mechanisms of resilience and vulnerability: implications for successful adaptation to extreme stress. Am. J. Psychiatr. 161, 195–216.
Chaudhury, D., Walsh, J.J., Friedman, A.K., Juarez, B., Ku, S.M., Koo, J.W., Ferguson, D., Tsai, H.C., Pomeranz, L., Christoffel, D.J., Nectow, A.R., Ekstrand, M., Domingos, A., Mazei-Robison, M.S., Mouzon, E., Lobo, M.K., Neve, R.L., Friedman, J.M., Russo, S. J., Deisseroth, K., Nestler, E.J., Han, M.H., 2013. Rapid regulation of depression-related behaviours by control of midbrain dopamine neurons. Nature 493, 532–536.
Cheng, J., Umschweif, G., Leung, J., Sagi, Y., Greengard, P., 2019. HCN2 channels in cholinergic interneurons of nucleus accumbens shell regulate depressive behaviors. Neuron 101, 662–672 e665.
Chevaleyre, V., Castillo, P.E., 2002. Assessing the role of Ih channels in synaptic transmission and mossy fiber LTP. Proc. Natl. Acad. Sci. Unit. States Am. 99, 9538–9543.
Chocyk, A., Dudys, D., Przyborowska, A., Majcher, I., Mackowiak, M., Wedzony, K., 2011. Maternal separation affects the number, proliferation and apoptosis of glia cells in the substantia nigra and ventral tegmental area of juvenile rats. Neuroscience 173, 1–18.
Chu, H.-y., Zhen, X., 2010. Hyperpolarization-activated, cyclic nucleotide-gated (HCN) channels in the regulation of midbrain dopamine systems. Acta Pharmacol. Sin. 31, 1036–1043.
D'Amato, F.R., Zanettini, C., Lampis, V., Coccurello, R., Pascucci, T., Ventura, R., Puglisi-Allegra, S., Spatola, C.A., Pesenti-Gritti, P., Oddi, D., Moles, A., Battaglia, M., 2011. Unstable maternal environment, separation anxiety, and heightened CO2 sensitivity induced by gene-by-environment interplay. PloS One 6, e18637.
Daskalakis, N.P., Bagot, R.C., Parker, K.J., Vinkers, C.H., de Kloet, E.R., 2013. The three-hit concept of vulnerability and resilience: toward understanding adaptation to early-life adversity outcome. Psychoneuroendocrinology 38, 1858–1873.
Di Segni, M., Andolina, D., Coassin, A., Accoto, A., Luchetti, A., Pascucci, T., Luzi, C., Lizzi, A.R., D'Amato, F.R., Ventura, R., 2017. Sensitivity to cocaine in adult mice is due to interplay between genetic makeup, early environment and later experience. Neuropharmacology 125, 87–98.
Di Segni, M., Andolina, D., D'Addario, S.L., Babicola, L., Ielpo, D., Luchetti, A., Pascucci, T., Lo Iacono, L., D'Amato, F.R., Ventura, R., 2019. Sex-dependent effects of early unstable post-natal environment on response to positive and negative stimuli in adult mice. Neuroscience 413, 1–10.
Di Segni, M., Andolina, D., Luchetti, A., Babicola, L., D'Apolito, L.I., Pascucci, T., Conversi, D., Accoto, A., D'Amato, F.R., Ventura, R., 2016. Unstable maternal environment affects stress response in adult mice in a genotype-dependent manner. Cerebr. Cortex 26, 4370–4380.
Di Segni, M., Andolina, D., Ventura, R., 2018. Long-term effects of early environment on the brain: lesson from rodent models. Semin. Cell Dev. Biol. 77, 81–92.
Di Segni, M., D'Addario, S.L., Babicola, L., Ielpo, D., Iacono, L.L., Andolina, D., Accoto, A., Luchetti, A., Mancini, C., Parisi, C., 2020. Xlr4 as a New Candidate Gene Underlying Vulnerability to Cocaine Effects. Neuropharmacology, p. 108019.
DiFrancesco, J.C., DiFrancesco, D., 2015. Dysfunctional HCN ion channels in neurological diseases. Front. Cell. Neurosci. 6, 174.
Douma, E.H., de Kloet, E.R., 2020. Stress-induced plasticity and functioning of ventral tegmental dopamine neurons. Neurosci. Biobehav. Rev. 108, 48–77.
Drysdale, A.T., Grosenick, L., Downar, J., Dunlop, K., Mansouri, F., Meng, Y., Fetcho, R. N., Zebley, B., Oathes, D.J., Etkin, A., Schatzberg, A.F., Sudheimer, K., Keller, J., Mayberg, H.S., Gunning, F.M., Alexopoulos, G.S., Fox, M.D., Pascual-Leone, A., Voss, H.U., Casey, B.J., Dubin, M.J., Liston, C., 2017. Resting-state connectivity biomarkers define neurophysiological subtypes of depression. Nat. Med. 23, 28–38.
Ellis, B.J., Boyce, W.T., Belsky, J., Bakermans-Kranenburg, M.J., van Ijzendoorn, M.H., 2011. Differential susceptibility to the environment: an evolutionary–neurodevelopmental theory. Dev. Psychopathol. 23, 7–28.
Fox, M.E., Lobo, M.K., 2019. The molecular and cellular mechanisms of depression: a focus on reward circuitry. Mol. Psychiatr. 24, 1798–1815.
Friedman, A.K., Juarez, B., Ku, S.M., Zhang, H., Calizo, R.C., Walsh, J.J., Chaudhury, D., Zhang, S., Hawkins, A., Dietz, D.M., Murrough, J.W., Ribadeneira, M., Wong, E.H., Neve, R.L., Han, M.H., 2016. KCNQ channel openers reverse depressive symptoms via an active resilience mechanism. Nat. Commun. 7, 11671.
Friedman, A.K., Walsh, J.J., Juarez, B., Ku, S.M., Chaudhury, D., Wang, J., Li, X., Dietz, D.M., Pan, N., Vialou, V.F., Neve, R.L., Yue, Z., Han, M.H., 2014. Enhancing depression mechanisms in midbrain dopamine neurons achieves homeostatic resilience. Science 344, 313–319.
Gershon, A., Sudheimer, K., Tirouvanziam, R., Williams, L.M., O'Hara, R., 2013. The long-term impact of early adversity on late-life psychiatric disorders. Curr. Psychiatr. Rep. 15, 352.
Gillies, G.E., Virdee, K., McArthur, S., Dalley, J.W., 2014. Sex-dependent diversity in ventral tegmental dopaminergic neurons and developmental programing: a molecular, cellular and behavioral analysis. Neuroscience 282, 69–85.
Grace, A.A., Onn, S.-P., 1989. Morphology and electrophysiological properties of immunocytochemically identified rat dopamine neurons recorded in vitro. J. Neurosci. 9, 3463–3481.
Guatteo, E., Rizzo, F.R., Federici, M., Cordella, A., Ledonne, A., Latini, L., Nobili, A., Viscomi, M.T., Biamonte, F., Landrock, K.K., Martini, A., Aversa, D., Schepisi, C., D'Amelio, M., Berretta, N., Mercuri, N.B., 2017. Functional alterations of the dopaminergic and glutamatergic systems in spontaneous alpha-synuclein overexpressing rats. Exp. Neurol. 287, 21–33.
Gururajan, A., Reif, A., Cryan, J.F., Slattery, D.A., 2019. The future of rodent models in depression research. Nat. Rev. Neurosci. 20, 686–701.
M.-H. Han, S.J. Russo, E.J. Nestler, Chapter 12 - molecular, cellular, and circuit basis of depression susceptibility and resilience, in: J. Quevedo, A.F. Carvalho, C.A. Zarate (Eds.) Neurobiology of Depression, Academic Press2019, pp. 123-136.
He, C., Chen, F., Li, B., Hu, Z., 2014. Neurophysiology of HCN channels: from cellular functions to multiple regulations. Prog. Neurobiol. 112, 1–23.
Heim, C., Binder, E.B., 2012. Current research trends in early life stress and depression: review of human studies on sensitive periods, gene-environment interactions, and epigenetics. Exp. Neurol. 233, 102–111.
Heim, C., Nemeroff, C.B., 2002. Neurobiology of early life stress: clinical studies. Semin. Clin. Neuropsychiatry 7, 147–159.
Heim, C., Newport, D.J., Mletzko, T., Miller, A.H., Nemeroff, C.B., 2008. The link between childhood trauma and depression: insights from HPA axis studies in humans. Psychoneuroendocrinology 33, 693–710.

Herbison, C.E., Allen, K., Robinson, M., Newnham, J., Pennell, C., 2017. The impact of life stress on adult depression and anxiety is dependent on gender and timing of exposure. Dev. Psychopathol. 29, 1443–1454.
Huang, Y.-Y., Liu, Y.-C., Lee, C.-T., Lin, Y.-C., Wang, M.-L., Yang, Y.-P., Chang, K.-Y., Chiou, S.-H., 2016. Revisiting the lamotrigine-mediated effect on hippocampal GABAergic transmission. Int. J. Mol. Sci. 17, 1191.
Isingrini, E., Perret, L., Rainer, Q., Amilhon, B., Guma, E., Tanti, A., Martin, G., Robinson, J., Moquin, L., Marti, F., Mechawar, N., Williams, S., Gratton, A., Giros, B., 2016. Resilience to chronic stress is mediated by noradrenergic regulation of dopamine neurons. Nat. Neurosci. 19, 560–563.
Kaufling, J., 2019. Alterations and adaptation of ventral tegmental area dopaminergic neurons in animal models of depression. Cell Tissue Res. 377, 59–71.
Kim, C.S., Johnston, D., 2018. A possible link between HCN channels and depression. Chronic Stress 2, 2470547018787781.
Kocsis, B., Li, S., 2004. In vivo contribution of h-channels in the septal pacemaker to theta rhythm generation. Eur. J. Neurosci. 20, 2149–2158.
Krashia, P., Martini, A., Nobili, A., Aversa, D., D'Amelio, M., Berretta, N., Guatteo, E., Mercuri, N.B., 2017. On the properties of identified dopaminergic neurons in the mouse substantia nigra and ventral tegmental area. Eur. J. Neurosci. 45, 92–105.
Krishnan, V., Han, M.-H., Graham, D.L., Berton, O., Renthal, W., Russo, S.J., LaPlant, Q., Graham, A., Lutter, M., Lagace, D.C., 2007. Molecular adaptations underlying susceptibility and resistance to social defeat in brain reward regions. Cell 131, 391–404.
Ku, S.M., Han, M.H., 2017. HCN channel targets for novel antidepressant treatment. Neurotherapeutics 14, 698–715.
Kumar, P., Goer, F., Murray, L., Dillon, D.G., Beltzer, M.L., Cohen, A.L., Brooks, N.H., Pizzagalli, D.A., 2018. Impaired reward prediction error encoding and striatal-midbrain connectivity in depression. Neuropsychopharmacology 43, 1581–1588.
Lammel, S., Ion, D.I., Roeper, J., Malenka, R.C., 2011 Jun. Projection-specific modulation of dopamine neuron synapses by aversive and rewarding stimuli. Neuron 970 (5), 855–862. https://doi.org/10.1016/j.neuron.2011.03.025. PMID: 21658580; PMCID: PMC3112473.
Lammel, S., Tye, K.M., Warden, M.R., 2014. Progress in understanding mood disorders: optogenetic dissection of neural circuits. Gene Brain Behav. 13, 38–51.
Ledonne, A., Mercuri, N.B., 2018. mGluR1-Dependent long term depression in rodent midbrain dopamine neurons is regulated by neuregulin 1/ErbB signaling. Front. Mol. Neurosci. 11, 346.
Lguensat, A., Bentefour, Y., Bennis, M., Ba-M'hamed, S., Garcia, R., 2019. Susceptibility and resilience to PTSD-like symptoms in mice are associated with opposite dendritic changes in the prelimbic and infralimbic cortices following trauma. Neuroscience 418, 166–176.
Liotti, M., Mayberg, H.S., 2001. The role of functional neuroimaging in the neuropsychology of depression. J. Clin. Exp. Neuropsychol. 23, 121–136.
Lo Iacono, L., Catale, C., Martini, A., Valzania, A., Viscomi, M.T., Chiurchiu, V., Guatteo, E., Bussone, S., Perrone, F., Di Sabato, P., Arico, E., D'Argenio, A., Troisi, A., Mercuri, N.B., Maccarrone, M., Puglisi-Allegra, S., Casella, P., Carola, V., 2018. From traumatic childhood to cocaine abuse: the critical function of the immune system. Biol. Psychiatr. 84, 905–916.
Luo, P., He, G., Liu, D., 2019. HCN channels: new targets for the design of an antidepressant with rapid effects. J. Affect. Disord. 245, 764–770.
Margolis, E.B., Toy, B., Himmels, P., Morales, M., Fields, H.L., 2012. Identification of rat ventral tegmental area GABAergic neurons. PloS One 7, e42365.
Marinelli, M., Rudick, C., Hu, X.-T., White, F., 2006. Excitability of dopamine neurons: modulation and physiological consequences. CNS Neurol. Disord. - Drug Targets 5, 79–97.
Martini, A., Cordella, A., Pisani, A., Mercuri, N.B., Guatteo, E., 2019. Neurotensin receptors inhibit mGluR I responses in nigral dopaminergic neurons via a process that undergoes functional desensitization by G-protein coupled receptor kinases. Neuropharmacology 155, 76–88.
Masrouri, H., Azadi, M., Semnanian, S., Azizi, H., 2020. Maternal deprivation induces persistent adaptations in putative dopamine neurons in rat ventral tegmental area: in vivo electrophysiological study. Exp. Brain Res. 238, 2221–2228.
Mayberg, H.S., Lozano, A.M., Voon, V., McNeely, H.E., Seminowicz, D., Hamani, C., Schwalb, J.M., Kennedy, S.H., 2005. Deep brain stimulation for treatment-resistant depression. Neuron 45, 651–660.
McDaid, J., McElvain, M.A., Brodie, M.S., 2008. Ethanol effects on dopaminergic ventral tegmental area neurons during block of I h: involvement of barium-sensitive potassium currents. J. Neurophysiol. 100, 1202–1210.
Meaney, M.J., Brake, W., Gratton, A., 2002. Environmental regulation of the development of mesolimbic dopamine systems: a neurobiological mechanism for vulnerability to drug abuse? Psychoneuroendocrinology 27, 127–138.
Medrihan, L., Umschweif, G., Sinha, A., Reed, S., Lee, J., Gindinova, K., Sinha, S.C., Greengard, P., Sagi, Y., 2020. Reduced Kv3. 1 Activity in Dentate Gyrus Parvalbumin Cells Induces Vulnerability to Depression. Biological Psychiatry.
Mercuri, N.B., Bonci, A., Calabresi, P., Stefani, A., Bernardi, G., 1995. Properties of the hyperpolarization-activated cation current Ih in rat midbrain dopaminergic neurons. Eur. J. Neurosci. 7, 462–469.
Migliore, M., Migliore, R., 2012. Know your current I h: interaction with a shunting current explains the puzzling effects of its pharmacological or pathological modulations. PloS One 7, e36867.
Morikawa, H., Paladini, C.A., 2011. Dynamic regulation of midbrain dopamine neuron activity: intrinsic, synaptic, and plasticity mechanisms. Neuroscience 198, 95–111.
Nederhof, E., Schmidt, M.V., 2012. Mismatch or cumulative stress: toward an integrated hypothesis of programming effects. Physiol. Behav. 106, 691–700.
Nestler, E.J., Barrot, M., DiLeone, R.J., Eisch, A.J., Gold, S.J., Monteggia, L.M., 2002. Neurobiology of depression. Neuron 34, 13–25.
Nestler, E.J., Carlezon Jr., W.A., 2006. The mesolimbic dopamine reward circuit in depression. Biol. Psychiatr. 59, 1151–1159.
Notomi, T., Shigemoto, R., 2004. Immunohistochemical localization of Ih channel subunits, HCN1–4, in the rat brain. J. Comp. Neurol. 471, 241–276.
Novick, A.M., Levandowski, M.L., Laumann, L.E., Philip, N.S., Price, L.H., Tyrka, A.R., 2018. The effects of early life stress on reward processing. J. Psychiatr. Res. 101, 80–103.
Okamoto, T., Harnett, M.T., Morikawa, H., 2006. Hyperpolarization-activated cation current (I h) is an ethanol target in midbrain dopamine neurons of mice. J. Neurophysiol. 95, 619–626.
Paladini, C.A., Roeper, J., 2014. Generating bursts (and pauses) in the dopamine midbrain neurons. Neuroscience 282, 109–121.
Patrono, E., Di Segni, M., Patella, L., Andolina, D., Valzania, A., Latagliata, E.C., Felsani, A., Pompili, A., Gasbarri, A., Puglisi-Allegra, S., 2015. When chocolate seeking becomes compulsion: gene-environment interplay. PloS One 10, e0120191.
Paxinos, G., Franklin, K.B., 2019. Paxinos and Franklin's the Mouse Brain in Stereotaxic Coordinates. Academic press.
Pechtel, P., Pizzagalli, D.A., 2011. Effects of early life stress on cognitive and affective function: an integrated review of human literature. Psychopharmacology (Berlin) 214, 55–70.
Pena, C.J., Kronman, H.G., Walker, D.M., Cates, H.M., Bagot, R.C., Purushothaman, I., Issler, O., Loh, Y.E., Leong, T., Kiraly, D.D., Goodman, E., Neve, R.L., Shen, L., Nestler, E.J., 2017. Early life stress confers lifelong stress susceptibility in mice via ventral tegmental area OTX2. Science 356, 1185–1188.
Pena, C.J., Smith, M., Ramakrishnan, A., Cates, H.M., Bagot, R.C., Kronman, H.G., Patel, B., Chang, A.B., Purushothaman, I., Dudley, J., Morishita, H., Shen, L., Nestler, E.J., 2019. Early life stress alters transcriptomic patterning across reward circuitry in male and female mice. Nat. Commun. 10, 5098.
Puglisi-Allegra, S., Ventura, R., 2012. Prefrontal/accumbal catecholamine system processes emotionally driven attribution of motivational salience. Rev. Neurosci. 23, 509–526.
Rincón-Cortés, M., Grace, A.A., 2017. Sex-dependent effects of stress on immobility behavior and VTA dopamine neuron activity: modulation by ketamine. Int. J. Neuropsychopharmacol. 20, 823–832.
Rokita, K.I., Dauvermann, M.R., Donohoe, G., 2018. Early life experiences and social cognition in major psychiatric disorders: a systematic review. Eur. Psychiatr. 53, 123–133.
Rothman, J.S., Silver, R.A., 2018. NeuroMatic: an integrated open-source software toolkit for acquisition, analysis and simulation of electrophysiological data. Front. Neuroinf. 12, 14.
Santarelli, S., Lesuis, S.L., Wang, X.-D., Wagner, K.V., Hartmann, J., Labermaier, C., Scharf, S.H., Müller, M.B., Holsboer, F., Schmidt, M.V., 2014. Evidence supporting the match/mismatch hypothesis of psychiatric disorders. Eur. Neuropsychopharmacol 24, 907–918.
Santarelli, S., Zimmermann, C., Kalideris, G., Lesuis, S.L., Arloth, J., Uribe, A., Dournes, C., Balsevich, G., Hartmann, J., Masana, M., 2017. An adverse early life environment can enhance stress resilience in adulthood. Psychoneuroendocrinology 78, 213–221.
Santoro, B., Shah, M.M., 2020. Hyperpolarization-activated cyclic nucleotide-gated channels as drug targets for neurological disorders. Annu. Rev. Pharmacol. Toxicol. 60, 109–131.
Santos-Vera, B., Vaquer-Alicea, A.D.C., Maria-Rios, C.E., Montiel-Ramos, A., Ramos-Cardona, A., Vazquez-Torres, R., Sanabria, P., Jimenez-Rivera, C.A., 2019. Protein and surface expression of HCN2 and HCN4 subunits in mesocorticolimbic areas after cocaine sensitization. Neurochem. Int. 125, 91–98.
Schmidt, M.V., 2011. Animal models for depression and the mismatch hypothesis of disease. Psychoneuroendocrinology 36, 330–338.
Schmitt, A., Malchow, B., Hasan, A., Falkai, P., 2014. The impact of environmental factors in severe psychiatric disorders. Front. Neurosci. 8, 19.
Shepard, R.D., Langlois, L.D., Authement, M.E., Nugent, F.S., 2020. Histone deacetylase inhibition reduces ventral tegmental area dopamine neuronal hyperexcitability involving AKAP150 signaling following maternal deprivation in juvenile male rats. J. Neurosci. Res. 98, 1457–1467.
Slattery, D.A., Cryan, J.F., 2017. Modelling depression in animals: at the interface of reward and stress pathways. Psychopharmacology (Berlin) 234, 1451–1465.
Song, S., Gleeson, J.G., 2018. Early life experience shapes neural genome. Science 359, 1330–1331.
Spyrka, J., Gugula, A., Rak, A., Tylko, G., Hess, G., Blasiak, A., 2020. Early life stress-induced alterations in the activity and morphology of ventral tegmental area neurons in female rats. Neurobiology of Stress 13, 100250.
Suter, B.A., Migliore, M., Shepherd, G.M., 2013. Intrinsic electrophysiology of mouse corticospinal neurons: a class-specific triad of spike-related properties. Cerebr. Cortex 23, 1965–1977.
Tan, A., Costi, S., Morris, L.S., Van Dam, N.T., Kautz, M., Whitton, A.E., Friedman, A.K., Collins, K.A., Ahle, G., Chadha, N., 2020. Effects of the KCNQ channel opener ezogabine on functional connectivity of the ventral striatum and clinical symptoms in patients with major depressive disorder. Mol. Psychiatr. 25, 1323–1333.
Tapia, M., Baudot, P., Formisano-Tréziny, C., Dufour, M.A., Temporal, S., Lasserre, M., Marquèze-Pouey, B., Gabert, J., Kobayashi, K., Goaillard, J.-M., 2018. Neurotransmitter identity and electrophysiological phenotype are genetically coupled in midbrain dopaminergic neurons. Sci. Rep. 8, 1–14.
Ting, J.T., Lee, B.R., Chong, P., Soler-Llavina, G., Cobbs, C., Koch, C., Zeng, H., Lein, E., 2018. Preparation of acute brain slices using an optimized N-Methyl-D-glucamine protective recovery method. JoVE. https://doi.org/10.3791/53825.

Torres-Berrio, A., Issler, O., Parise, E.M., Nestler, E.J., 2019. Unraveling the epigenetic landscape of depression: focus on early life stress. Dialogues Clin. Neurosci. 21, 341–357.
Trombin, F., Gnatkovsky, V., de Curtis, M., 2011. Changes in action potential features during focal seizure discharges in the entorhinal cortex of the in vitro isolated Guinea pig brain. J. Neurophysiol. 106, 1411–1423.
Tye, K.M., Mirzabekov, J.J., Warden, M.R., Ferenczi, E.A., Tsai, H.C., Finkelstein, J., Kim, S.Y., Adhikari, A., Thompson, K.R., Andalman, A.S., Gunaydin, L.A., Witten, I. B., Deisseroth, K., 2013. Dopamine neurons modulate neural encoding and expression of depression-related behaviour. Nature 493, 537–541.
Ungless, M.A., Magill, P.J., Bolam, J.P., 2004. Uniform inhibition of dopamine neurons in the ventral tegmental area by aversive stimuli. Science 303, 2040–2042.
Ventura, R., Coccurello, R., Andolina, D., Latagliata, E.C., Zanettini, C., Lampis, V., Battaglia, M., D'Amato, F.R., Moles, A., 2013. Postnatal aversive experience impairs sensitivity to natural rewards and increases susceptibility to negative events in adult life. Cerebr. Cortex 23, 1606–1617.
Villarroel, H.S., Bompolaki, M., Mackay, J.P., Tapia, A.P.M., Michaelson, S.D., Leitermann, R.J., Marr, R.A., Urban, J.H., Colmers, W.F., 2018. NPY induces stress resilience via downregulation of Ih in principal neurons of rat basolateral amygdala. J. Neurosci. 38, 4505–4520.
Yan, S., You, Z.-L., Zhao, Q.-Y., Peng, C., He, G., Gou, X.-j., Lin, B., 2015. Antidepressant-like effects of Sanyuansan in the mouse forced swim test, tail suspension test, and chronic mild stress model. Kaohsiung J. Med. Sci. 31, 605–612.
Yang, C., Yan, Z., Zhao, B., Wang, J., Gao, G., Zhu, J., Wang, W., 2016. D2 dopamine receptors modulate neuronal resonance in subthalamic nucleus and cortical high-voltage spindles through HCN channels. Neuropharmacology 105, 258–269.
Zhang, H., Chaudhury, D., Nectow, A.R., Friedman, A.K., Zhang, S., Juarez, B., Liu, H., Pfau, M.L., Aleyasin, H., Jiang, C., Crumiller, M., Calipari, E.S., Ku, S.M., Morel, C., Tzavaras, N., Montgomery, S.E., He, M., Salton, S.R., Russo, S.J., Nestler, E.J., Friedman, J.M., Cao, J.L., Han, M.H., 2019. alpha1- and beta3-adrenergic receptor-mediated mesolimbic homeostatic plasticity confers resilience to social stress in susceptible mice. Biol. Psychiatr. 85, 226–236.
Zhong, P., Vickstrom, C.R., Liu, X., Hu, Y., Yu, L., Yu, H.G., Liu, Q.S., 2018. HCN2 channels in the ventral tegmental area regulate behavioral responses to chronic stress. Elife 7.